Vinh Nguyen

FUNCTIONALIZATION OF GRAPHENE FROM ELECTROCHEMICAL EXFOLIATION AND FLUOROGRAPHENE REDUCTION FOR USE IN POLYURETHANE COMPOSITE MATERIALS

Thesis
CENTRIA UNIVERSITY OF APPLIED SCIENCES
Environmental Chemistry and Technology
September 2019

Centria University of Applied Sciences	Date September 2019	Author Vinh Nguyen
Degree programme Environmental Chemistry and Technology		
Name of thesis FUNCTIONALIZATION OF GRAPHENE FROM ELECTROCHEMICAL EXFOLIATION AND FLUOROGRAPHENE REDUCTION FOR USE IN POLYURETHANE COMPOSITE MATERIALS.		
Instructor Prof. Kim Daasbjerg & Assoc. Prof. Steen Uttrup Pedersen		**Pages** 41+14
Supervisor Jana Holm		

Composite materials are employed in a wide variety of markets, including aerospace, architecture, automotive, energy, infrastructure, marine, military, and sports and recreation, due to the significantly different and advanced physical or chemical properties, compared with the individual components used for making the composites. Based on the desire products, focusing on strength and conductivity, functional graphene is used to combine with polyurethane (PUR) to make a new composite material for industries. Two types of functional graphene were discussed and studied in this thesis, which are rendered from exfoliated graphene (EG) and fluorographene (FG) methods. In EG, the functional graphene was produced in only one step by using chemical exfoliation with diazonium salts in the electrolyte, which was employed as the functional groups on graphene sheets. However, functional graphene from FG was prepared within two steps, consisting of cyanidation fluorographene and amine conversion. The yield of functionalization of FG is much higher than the functionalization of EG.

To utilize the graphene properties in the composites, growing polymer brushes from functional groups on graphene is suggested and carried out for the EG; the process called as polymerization. The composite material samples with graphene presence is stiffer than the pure PUR sample, meaning the efficiency of graphene. In particular, the functional graphene presents the highest quality in the composite, while the composite from polymerized graphene is a bit stronger than the one mixed only with graphene. Besides, the concentration of graphene content in composite could influence the strength of the composite, in which the higher the concentration of the graphene content is, the stiffer the composite becomes.

Key words
Graphene, fluorographene, electrochemistry, functional graphene, amine conversion.

ACKNOWLEDGEMENT

Firstly, I would like to express my appreciation to Prof. Kim Daasbjerg for gifting me the chance of working on this project and guiding the direction.

I would like to express my gratitude to Associate Professor Steen Uttrup Pedersen for his extraordinary ideas and discussions during the project work.

I would like to thank Andreas Brunsgaard Laursen and Sisse Holm Rasmussen for always being there to help and discuss about Raman spectroscopy / XPS data analysis and the issues of project.

I would like to thank Marcel Ceccato for teaching and guiding me detail about using the XPS data analyses for the project.

I would like to thank Magnus Hansen-Felby, Stefan Urth Nielsen and Asger Holm Agergaard for suggesting and helping me in choosing chemicals and implementing reactions in the project.

I would like to thank Jonas Greibe Hansen for his assistance in NMR measurement

I would like to thank Hongqing Liang, Xinming Hu, Sunirmal Pal and Magnus Haugaard Rønne for the discussion and advise the reactions in project.

I would like to thank deeply to all people in Organic Surface Chemistry group at Aarhus University for being always willing to help me and making me feel at home.

I would like to thank Jana Holm and Hubert Spiz for being my coordinators between two Universities in this project.

Lastly, I would pay my gratitude to Erasmus organization for giving a grant to me in this project.

CONCEPT DEFINITIONS

AFM	Atomic Force Microscopy
ATRP	Atom transfer radical polymerization
DMF	Dimethylformamide
EG	Exfoliated graphene
EG-Cl	Functional graphene with chloride group
EG-EOH	Functional graphene with ethanol group
EG-OH	Functional graphene with hydroxide group
EG-P	Functional graphene with brushes
FG	Flourographene
FG-CN	Functional flourographene with cyano group
FG-L	Functional fluorographene undergone with long sonication
FG-NH_2	Functional flourographene with amine group
FG-S	Functional fluorographene undergone with short sonication
FG-TBA	Functional fluorographene undergone with Tetrabutylammonium cyanine
FG-wet	Functional fluorographene undergone with wet solvent
HEMA	(Hydroxyethyl)methacrylate
IR	Infrared spectroscopy
LAH	Lithium aluminum hydride
MNP	N-Methyl-2-pyrrolidone
PUR	Polyurethane
SET-LRP	Single electron transfer – living radical polymer
TBA	Tetrabutylammonium cyanine
XPS	X-ray Photoelectron Spectroscopy

1 INTRODUCTION

Living in the modern and developed world, every superior and innovative gadgets / machines are invented and manufactured, leading to the request of new advanced materials, which possess such properties, such as less weight, higher conductivity, greater strength and so on. By fusing different compounds to one, composite materials, also known as submaterials, are employed as the material source in industries to render goods and products, which have better performance than the previous material (van Suchtelen 1972) due to their all possible physical quantities from participating materials. Graphene is one of outstanding candidates for composite material, due to its prominent properties, including high strength, high conductivity, lightweight, and flexibility (Brownson and Banks 2014; Lee. 2008a; Stormer, KimSikes, Fudenberg, Hone, Bolotin, Jiang, Klima. 2008; Yingchang. 2019). By combining graphene and polymers for making composite materials, these types of materials could provide diverse features used in various applications, namely biosensors, batteries, electronics, etc. The advantages of graphene could be exposed fully in the composite, since the graphene sheets are dispersed in the polymer matrix (Noh. 2015). However, the graphene sheets are easy to get aggregated into many layers and form back to graphite, hence functionalizing moieties on graphene sheets is suggested and carried out, in order to separate and maintain the graphene sheets.

In this project, functionalization graphene was targeted and prepared as the key material for making composite material by mixing with the commercial polymer, polyurethane (PUR). By using functional graphene in composites, the composite material could be improved and enhanced in strength. Two functionalization graphene methods were focused and implemented, namely exfoliated graphene (EG) from graphite and derivation of cyanographene from fluorographene (FG). The reason of using EG is because it has been reported successfully in producing large scale with low cost and simple, while FG is promising in a high yield in functionalization on graphene. In EG, by employing electrochemistry, graphite could be exfoliated to graphene and functionalized benzyl alcohol group from the pursuant diazonium salt, all in one step. In another method, graphite fluoride was undergone in sonication for the pretreatment step to produce FG. Then, the FG was transferred to defluorination and functionalization process, where both happened simultaneously, by reacting with cyanide salts. In anime conversion process the cyanided fluorographene (FG-CN) was treated with lithium aluminum hydride (LAH) to reduce nitrile to amine.

The method for graphene functionalization from FG is much more efficient than the functional graphene from EG; however, in exchange, the properties of graphene sheet would be lower in the product from

FG, compared with the one from EG. Depending on the goal of product utilities, the number of functional groups on graphene could be deemed as the compromise between full graphene activities or partial graphene characters. Moreover, the functional graphene from EG was used to grow polymer brush, which was supposed to support the linking between the graphene sheet and the commercial polymers in the composite material. Hence the graphene of EG was carried out with two more processes, including chlorination and polymerization, which is employed to build the brushes on functional group of graphene.

The composite material was made from the product of EG method and polyurethane (PUR). The stiffness of composites having graphene content displays higher quality than the one with only PUR, proving the effect of graphene to the composite material. The product from functional graphene is the stiffest material, while the materials polymerized graphene is little stronger than the one mixed with blank graphene. The concentration of graphene content in composites also effects to the hardness of the material, by which the more graphene content in sample is the stiffer the material gains. Besides, the higher number of functional groups on graphene is expected to render the stronger composite material.

2 BACKGROUND OF THEORIES

In this thesis work, two functionalization methods were studied and implemented, namely graphene exfoliation and fluorographene. The products from the two methods were analyzed and compared to show which one is more efficient in functionalization. At the end of the project, the functional graphene was employed to make a composite material with polyurethane (PUR) a commercial polymer. The composite material could be used for diverse application, such as in aircraft and car structure, in infrastructure and material for architectures

2.1 Graphene background

The graphene was discovered by Andre Geim and Konstantin Novoselov in 2004 at the University of Manchester (Novoselov, Geim, Morozov, Jiang, Zhang, Dubonos, Grigorieva 2004); the graphene was initially disengaged from graphite by Scotch tape and the consequence of the work was rewarded the Nobel Prize in Physics in 2010 (Gupta and Taguchi 1982). Graphene is a 2D man-made material which has monolayer of honeycomb lattice, having sp^2 hybridized carbon atoms. Graphene is one single sheet detached from graphite, which is one of the carbon allotropes, as diamond, amorphous carbon, buckyballs and nanotubes, see Figure 1. Graphene has black color, distinguished from sliver-metallic color of graphite. Graphene is known as the strongest material in 2008 with a tensile strength of 130 GPa (Lee, Changgu, Xiaoding, Jeffrey and James Hone. 2008b), the best conductor of electricity (Stormer. 2008) as well as the best conductivity of heat at room temperature (Teweldebrhan. 2008), besides, the flexibility of graphene is determined via the effective elastic modulus with 2.4 TPa (Hartmann. 2013).

The graphene with a few layers can still gratify the quality of the graphene properties, so that industries and companies also could use the few-layers graphene instead of a single layer graphene, which is synthesized difficultly and costly. The ideal of 2D sheet-like graphene, also called multi-layer graphene, consists between 2 to 10 well-defined stacked layers (Enoki, Koratkar, Tascon. 2013). The properties of graphene can be lost if the number of graphene sheets is more than 10 layers. Furthermore, based on the distance among layers graphene planes which is 0.335 nm, the number of graphene sheets from graphene flake can be derived from the thickness of the flake (Brownson and Banks 2014). The thickness of a single graphene layer can be disregard due to the same as one atom diameter.

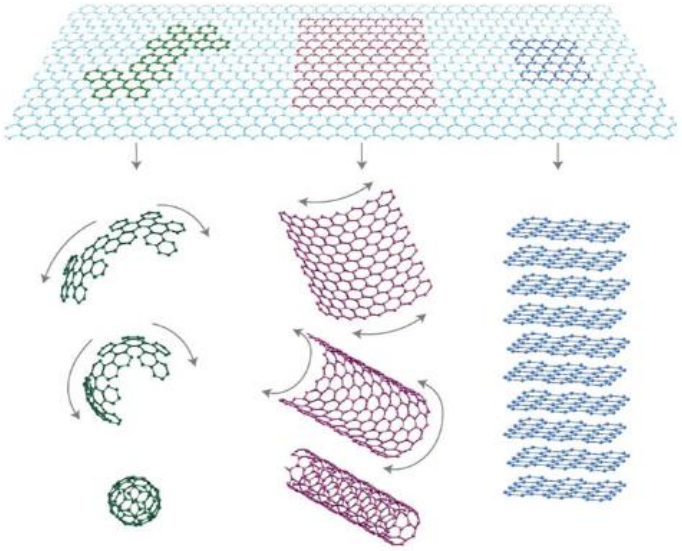

FIGURE 1: Mother of all graphitic forms. Graphene is a 2D building material for carbon materials of all other dimensionalities(Brownson and Banks 2014).

2.2 Electrochemistry exfoliation

In the electrochemistry system, there are three component parts, namely two electrodes and electrolyte (Oldham 2010; Hibbert 1993). The electrolyte is a conducting phase, a solution, where ions can be dissolved. The two electrodes are two solid plates or lumps of materials, which are introduced into the electrolyte; these two electrodes are called as cathode and anode, wherein cathode exhibits the reduction and anode performs the oxidation. The working principle of electrochemistry is based on electron transfer behavior among molecules and ions inside the solution, by which the material from the anode is driven to the cathode. The reaction is set off by employing an external voltage (Bond, Fleischmann, and Robinson 1984), which play the role of electrons stimulation factor (Hibbert 1993) to trigger the movement of the electrons inside the system. The ions in the electrolyte are attracted by the opposite charge electrodes, based on faradaic current (Biesheuvel and Dykstra 2018; Wu, Jingjie, Sharma, Harris, and Xiao. 2014).

One of the first publications of electrochemistry method for the preparation of graphite intercalation compound was released in the early 1970s (Besenhard 1976). However, until recent years, after graphene exploration in 2004 (Gupta and Taguchi 1982), the electrochemistry method has been focused into the synthesis of graphene and this method has become one of the most effective graphene production methods, which is fast, simple and low-cost in exfoliated graphene production (Ling, sWestwood 2016). Underlying on electrochemical techniques, namely bulk technique and interfacial technique, the graphite

can be incessantly intercalated, due to ionic species driven, under voltage impact (Achee, Thomas C. et al. 2018; Yang. 2019). Then, the graphite is expanded and exfoliated into the bulk of electrolyte to produce graphene. The electrochemical reactions only occur between the interfaces of electrodes and the solution, hence, the electrodes will be reduced and worn away. During the reaction, the reactant on the surface decreases as the product increases.

2.3 Analysis techniques

There are mainly three technique employed to identify the success of the reactions and experiments. Due to the special physical properties of graphene, there are not many spectroscopies that can be used for characterizing the graphene products. Thus, in this report, Raman spectroscopy and X-ray Photoelectron spectroscopy are employed for the measurement.

2.3.1 Raman spectroscopy

Raman spectroscopy is a spectroscopic technique which is based on inelastic scattering of monochromatic light. Laser sources is usually employed as the source light for Raman machine; the Raman technique is used to observe the rotation and vibration of molecules to identify the sample contents. In Raman spectroscopy concept, the inelastic scattering of monochromatic light is illustrated by the change phenomenon of photons frequency in monochromatic light, when the light is scattered by molecules (Bumbrah and Sharma 2016).

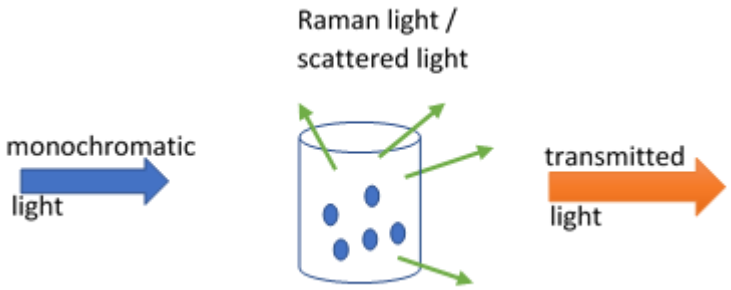

FIGURE 2: Demonstration of Raman principle (Bumbrah and Sharma 2016)

In detail of Raman principle, a monochromatic laser beam is used to illuminate into the sample which hits to the molecules of sample and originates a scattered light. Due to the different frequency from that

incident light, the Raman spectrum can be constructed (Bumbrah and Sharma 2016). In Figure 2, the Raman effect is depicted as the idea of Raman light collection, where the monochromatic light is introduced into the sample, the light will get absorbed; only the major portion could pass through, called transmitted light. The absorbed light in the end will be released and scattered by the sample in all the directions; those scattered lights are collected by detectors/sensors at the right angle and compared with the incident light, see in Figure 3. The incident light provides a source into the sample, then the molecules in the sample will get excited from ground state and up virtual state. At this state, the light is scattered back either the same energy to the ground state, called Rayleigh scattering, or less energy and end up in Stoke line, where Stoke photon is measured. This is caused by the molecule which absorbed the light; by that the molecule is identified by subtraction between incident light and Stoke photon. There is also Anti-Stoke line, which is created when the molecule in Stoke line get excited by a new incident light raises up to the higher virtual state and goes back to the ground state (Flemban 2017).

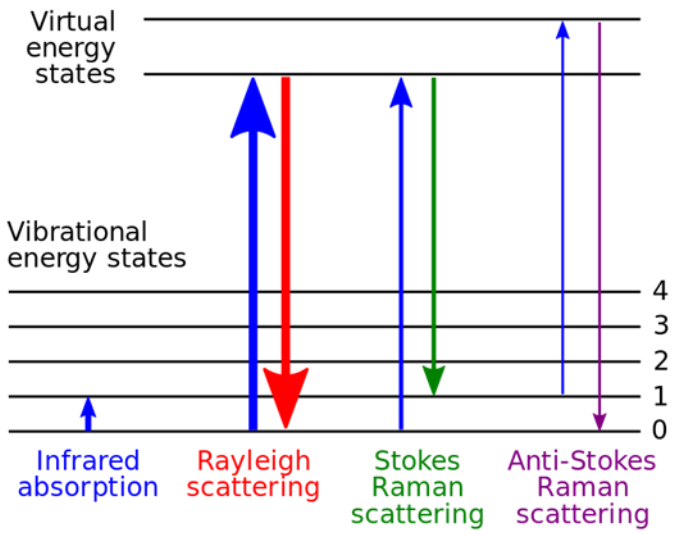

FIGURE 3: In Raman spectroscopy different scattering displays, where Stokes scattering is the one, providing the desire information (Flemban 2017).

Raman spectroscopy is a powerful tool for characterizing the structures of graphene. The Raman technique includes quantifying the number of defects on the graphene sheet and the number of graphene layers. The functional compounds embedded into the graphene will appear as an increase in sp^3 hybridized carbon; this change can be identified in a Raman spectrum as defects. Due to the electronic structure of graphene, which can be captured by Raman, the increase of layers of graphene causes to the changes in spectrum, leading to establishing the number of single layers graphene (Flemban 2017).

In Figure 4, all sp^2 carbon lattice have some common characteristics in Raman spectroscopy, due to its pi bonds, by which the disorder in sp^2 network could be detected (Dresselhaus, Mildred, Jorio, Hofmann, Dresselhaus, and Saito. 2010). The two dominant peaks in graphene are the G and G' peaks. The G band is demonstrated by the stretches of C-C around wavenumber 1584 cm^{-1} which is influenced sensitively by chemically doping the graphene, resulting to straining and upshifting which is another important aspect of characterizing this band (Englert, Jan , Vecera, Knirsch, Schäfer, Hauke, and Hirsch. 2013). While the G' peak, also called as 2D peak, is located in range 2500-2800 cm^{-1} and it is helpful for determination of graphene layers by probing for differences in sp^2 carbon systems. That shows the changes in both shape and position depending on number of layers Dresselhaus. 2009). The 2D peaks is formed by the second order of zone-boundary phonons, which is necessary to provide to the measurement of graphene layers (thickness). Because the first order zone-boundary phonon is low and not sufficient for the Raman fundamental selection rule. Finally, there one more concerned peak in graphene is the D band, spotted around 1345 cm^{-1}, which shows the quantity of defects on graphene or disorder of the sample (Dresselhaus et al. 2010). In addition, there are also peaks called D' and D+D', which are which are overtones.

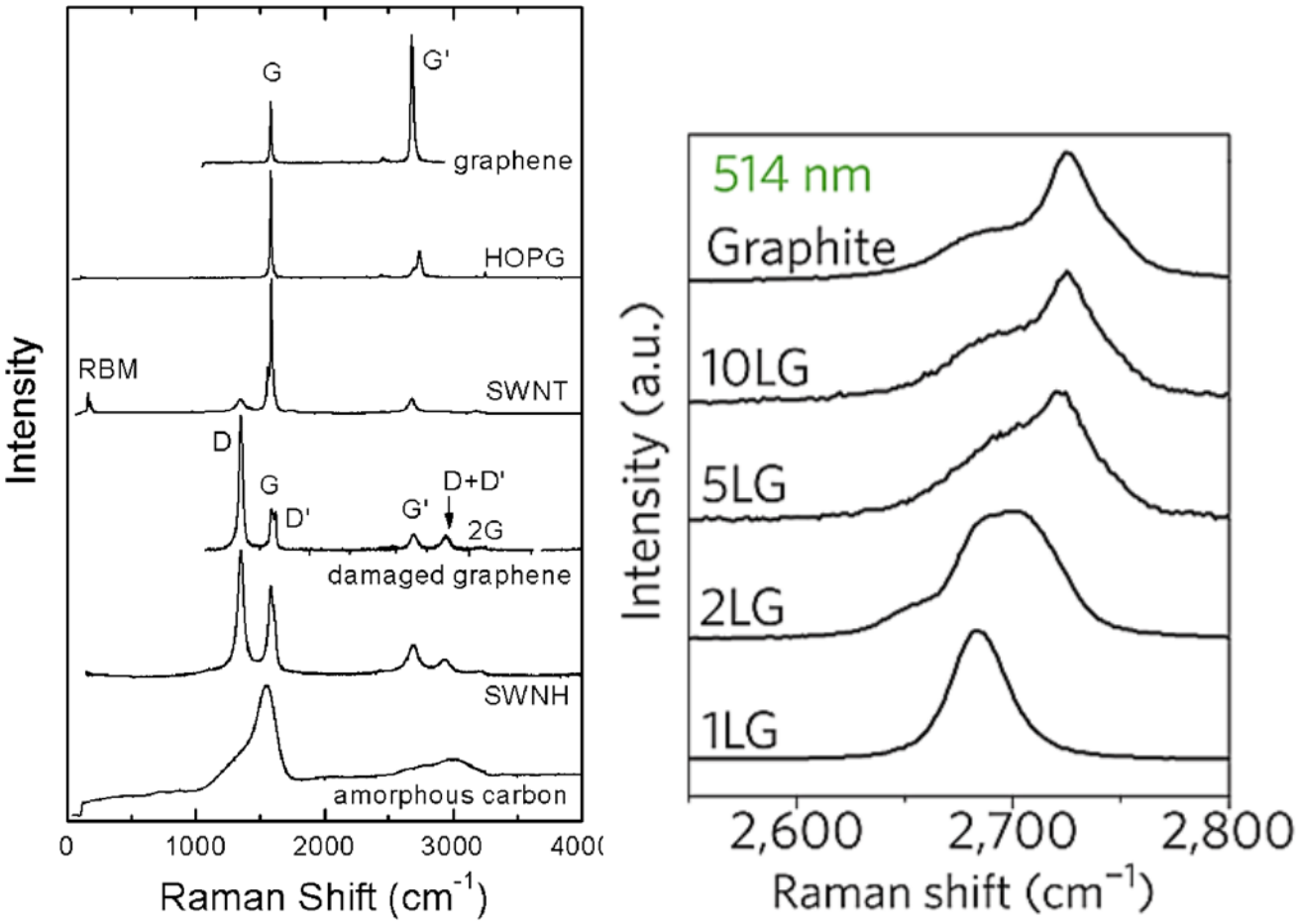

FIGURE 4: Left: Difference in Raman spectra from different kinds of graphene/graphite (Dresselhaus et al. 2010). Right: The changes in the 2D peak as a function of layers of graphene (LG). These measurements are done with a laser with a wavelength of 514 nm (Ferrari and Basko 2013).

The defects in sp^2 carbon systems using Raman Spectroscopy is quantified by comparing the intensity of the defect-induced D band (I_D) with the intensity of the G band (I_G), i.e. the I_D/I_G ratio. The more disorder and defects on graphene is, the larger D peak is showed; this leads to the higher in ratio of two intensity peaks (Dresselhaus et al. 2010). A model found by Luchese et al is applied to determine the quantity of the defects on graphene induced by ion bombardment (Jorio, Ado, Ferreira, Cançado, Achete, and Capaz. 2009) by observing a damage region with radius r_S and a second region with radius r_A, see in Figure 5, the defect is defined by the method.

FIGURE 5: The definition of the "structurally disordered" S-region(red) and the "activated" Aregion (green), provided from .(Jorio, Ferreira, Stavale, Achete, Capaz, Moutinho, Lombardo, Kulmala, and Ferrari. 2011).

The damaged region is presented as using two regions, namely the "structurally disordered" S-region with the radius r_S and the "activated" A-region with radius r_A; the A region is structurally intact, however, it gets effected by the damage done to the S region. The model lately was expanded by (Kuila et al. 2012) to work on covalent functionalization of graphene by adjusting smaller the two radii r_S and r_A, because there is much less damage on graphene by covalent bonding rather than ion bombardment. The calculation, in equation 1, is used to estimate the defects; where r_S = 0.07 nm and r_A = 1.0 nm, which are adjusted values used in this report.

$$\frac{I_D}{I_G} = C_A \frac{r_A^2 - r_S^2}{r_A^2 - 2r_S^2}\left[\exp\left(-\frac{\pi r_S^2}{L_D^2}\right) - \exp\left(-\frac{\pi\left(r_A^2 - r_S^2\right)}{L_D^2}\right)\right] + C_S\left[1 - \exp\left(-\frac{\pi r_S^2}{L_D^2}\right)\right] \quad (1)$$

Furthermore, the number of graphene layers in the samples could be counted in Raman spectroscopy by using a model made by (Paton, Keith R., Eswaraiah Varrla, Claudia Backes, Ronan J. Smith, Umar Khan, Arlene O'Neill, Conor Boland, et al. 2014). The formula for Raman metric, M, is depicted from the intensity ratios of two positions on the 2D-peaks, show in equation 2

$$M = \frac{I_{graphene}\,/I'_{graphene}}{I_{graphite}\,/I'_{graphite}} \quad (2)$$

where, I is intensity of the 2D peak position in the samples and, I' is the intensity peak at position P before 2D peak, where P position equals the subtracted 2D position with 30 cm^{-1}. The number of graphene layers, N_G, can be estimated using the equation (3).

$$N_G = 10^{0.84M+0.45M^2} \quad (3)$$

2.3.2 Sub-heading X-ray photoelectron spectroscopy

X-ray photoelectron spectroscopy (XPS) is a surface characterization technique, measuring the elemental composition based on their electronic properties, with a depth of investigation from 1 to 10 nm on the surface of the material. XPS measurement not only shows all chemical element presence in the material, but also indicate the chemical bonds, exiting among these elements, except hydrogen and helium. By irradiating X-ray beams to the sample in ultrahigh vacuum, the light is absorbed completely by the core electron of an atom. Then some of the core electrons are escaped out of the material if the photon energy (h) is large enough, due to the photoelectric effect(Greczynski and Hultman 2019). The binding energy of the core electron is given by the Einstein relationship, see in equation 4.

$$E_{bind} = hv - E_{kin} - \Phi_{spec} \quad (4)$$

Where hv is the X-ray energy, Φ_spec is the work function of the spectrometer used in the measurement and Ekin is the kinetic energy of photoelectron. The binding energy depends mostly on the Z number of the atom and abundant chemical for determining both elemental composition and chemical state of the elements. The binding energy should be calibrated with an internal reference peak, when the core binding energies shifts to higher values; the C 1s peak with the binding energy of 284.8eV is commonly used as the reference for calibration. There are two section in XPS measurement, including XPS survey spectrum and high-resolution XPS scan spectra. In XPS survey, the quantity and identity of each element can be defined by specific peak from spectra. While the high-resolution scan spectra could verify the types of bonds among elements in the samples by fitting peaks into the graph and recognized the position of those peaks(Kaciulis. 2014).

2.3.3 Atomic force microscopy (AFM)

Atomic force microscopy (AFM) is a sensitive surface probe type of scanning probe microscopy for studying samples from microscale, e.g. bacteria, DNA chains, to nanoscale, such as graphene. There are three types of AFM mode, namely contact mode, non-contact mode and tapping mode which is employed in this project. The AFM probes samples by a cantilever with a sharp tip which surfs and sweeps over the surface of samples. The tip, at first, is lowered down to proximity of a sample surface. when the tip crossing the surface, a deflection from the cantilever oscillation is created based on Hooke's law, resulting to sketching the image of the surface through a laser beam, see in Figure 6.

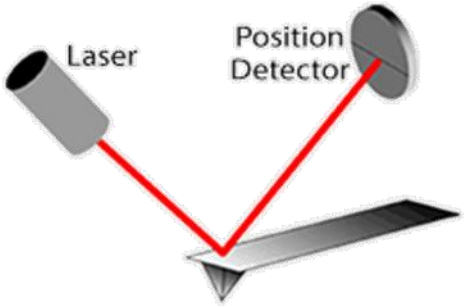

FIGURE 6: Illustration of the laser beam deflection for atomic force microscopes (Nanoscience instrucment)

In this project, the usage of AFM is to measure the thickness of the flakes, which can represent approximately the number of layers of the graphene after exfoliation process; the samples are often prepared by either spin coating or dipping substrate. The thickness of multiple graphene layers includes both number of functional graphene layers and potential solvent contaminating among layers, hence the thickness of one single layer from functional graphene is more than 0.34 nm (theoretical pure one graphene layer) (Dorn, Lange, Chekushin, Severin, and Rabe. 2010). Besides, there are some other complications influencing to the measurement (Jussila, Henri, Owen, Yang, Hu, Aksimsek, Granqvist, Lipsanen, Howe, Sun, and Hasan. 2017) and also the methods and types of AFM are taken into account of estimating the true thickness of single graphene layer (Stapleton, Andrew, Shearer, Gibson, Slattery, and Shapter. 2016).

2.4 Graphene exfoliation

Graphene studies has been focused intensively for a decade. There are many different methods and techniques published such as liquid-phase exfoliation (Hernandez, Yenny, Nicolosi, Lotya, Blighe, Sun, De, McGovern. 2008), chemical vapor deposition (Jacobberger, Robert, Machhi, Wroblewski, Taylor, Daniel, and Arnold. 2015) and electrochemical exfoliation (Achee et al. 2018; Parvez, Khaled, Wu, Li, Liu, Graf, Feng, and Müllen. 2014; Yingchang Yang et al. 2019). Unfortunately, graphene is a low reactive material, thus, it is difficult to make the connection between graphene sheets with other materials, due to graphene inertness character. Therefore, functionalizing graphene with and active compound is attracting to the scientist, because it is not only support graphene to associate with other material, functional group can also enhance the properties for the materials cooperation. Due to economic consideration, there are only some outstanding methods that can exfoliate the graphite to graphene and functionalize them as the same pot, such as mechanism method from (Wu, Hang, Weifeng Zhao, Huawen Hu, and Chen. 2011), and electrochemical exfoliation method from (Ossonon and Bélanger 2016), which is also the main idea for EG in this project.

2.4.1 Functionalizing graphene

The electrochemistry exfoliation technique was employed for exfoliating and functionalizing graphene at the same time by using a diazonium salt, inspired by an article from Professor Daniel Belangér from Université du Québec à Montréal (Ossonon and Bélanger 2016). The procedure is similar with the normal graphene exfoliation process, in which 0.1 M of H_2SO_4 solution is used as electrolyte and a constant 10V DC potential is applied to transmit the anions in solution into grain boundaries (Shang, Westwood 2016; Parvez, Khaled, Yang, Feng, and Müllen. 2015), see in Figure 7. Because of the positive charge on graphene, the sulphate ion with negative charge could easily intrude to among graphene layers and intercalate graphite to the graphene platelets. Thus, the reaction is in an oxidative environment.

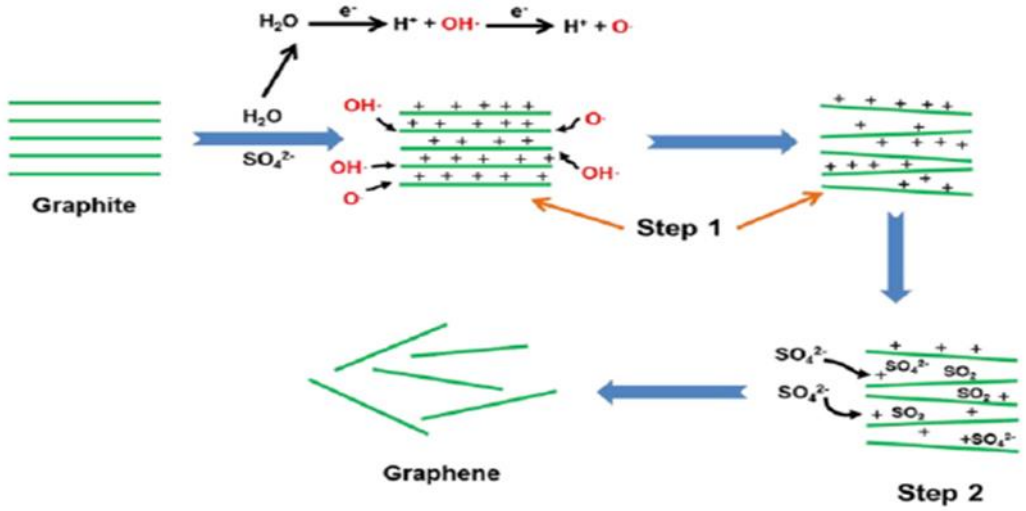

FIGURE 7: Electrochemical exfoliation mechanism to obtain graphene from graphite (Parvez et al. 2015).

The key for functionalization on graphene is adding an amount of diazonium salt into the electrolyte to react with the exfoliated graphene sheets; the idea also was applied in different type of salt, for instance amino group, reported by (Gu, Yong, Hsieh, Yuan, Hsueh, and Gandomi. 2018). The diazonium salt with tetrafluoroborate anion were used in the experiments. The idea using the diazonium salt is to apply the aryl radical at the dinitrogen position on the benzene ring after reducing the group dinitrogen by providing a free electron to the salt solution; the process known as dediazonation, see in Figure 8. This radical is very reactive, and it can incorporate spontaneously with the delocalized electron on the surface of graphene and that creates a covalent bond (Ossonon and Bélanger 2017), making the defect, on the graphene structure. In the reaction, graphene plays as the reduction agent role. Furthermore, due to the presence of functional salt on the graphene, the graphene sheet will be kept separately to each other and against the Van der Waals force, which force causes graphene layers to be packed together to form graphite. However, the mechanism of functionalization of diazonium salts is not totally understood, because the diazonium salts are grafted in reductive environments (Allongue et al. 1997), contracting with the condition for the process.

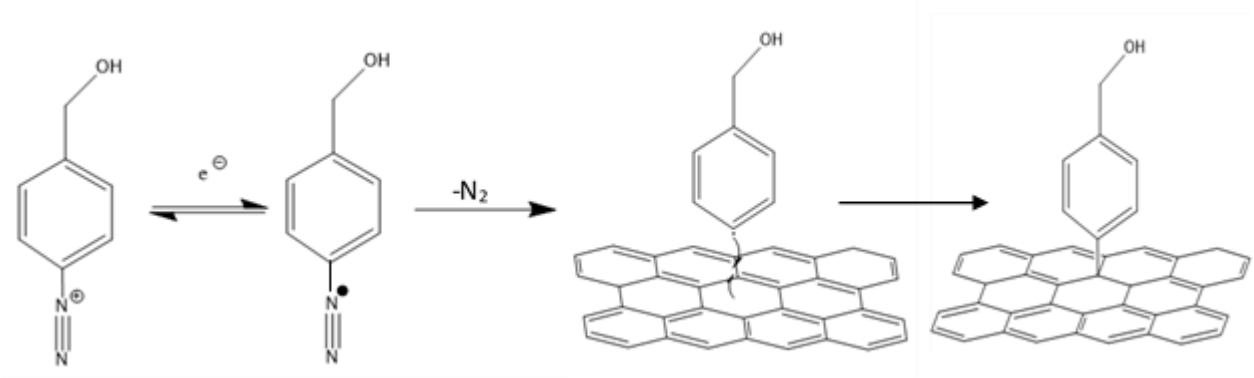

FIGURE 8: Proposed scheme of functionalization on graphene, where the diazonium salt releases nitrogen bond to localizes on graphene surface, based on the article reaction (Gu et al. 2018)

Besides, the benzyl chloride diazonium salt was not employed, due to the risk of the aryl radicals doing a chloride abstraction from the benzyl moiety during the exfoliation step, making the benzyl functional group on graphene sheet, undesired product from the functionalization process. Therefore, the tedious process, which employed benzyl alcohol in functionalization and chlorination for converting hydroxide (OH^-) to chloride (Cl^-) on functional group, was suggested and implemented. In the sequence, the functional group on graphene could be used for the polymerization process before employing in composite materials production.

2.4.2 Chlorination for functional graphene

Chloride is one of the crucial intermediates in organic synthesis and the chlorination process for the chlorine conversion is an important synthetic procedure. In this project, chlorine is, then, nominated to play the initiator role for the polymer reaction. The conversion of chlorine into the corresponding alcohol group on benzyl alcohol from functional graphene was investigated. There are many reagents, such as hydrochloric acid, phosphorus halides, cyanuric chloride and thionyl chloride, could be used to the chlorination from alcohols in compounds (Sun, Peng, Niu, Wang, Li. 2008), however on the surface reaction, it is harsh to get the success. Thus, the thionyl chloride reaction is used to chlorinate the functional graphene, inspired by the report succeeding in brominating alcohol on surface via thionyl bromide (Nielsen, Koefoed, Lund, Daasbjerg and Pedersen. 2016).

Chlorination by thionyl chloride is one of the basic conversion techniques available in most of organic chemistry textbooks. A possible mechanism for the formation of benzyl chlorides from benzyl alcohol is depicted in the Figure 9. The first step is the displacement between nucleophilic oxygen atom of the

alcohol and chloride ion from thionyl chloride, forming a protonated alkyl chlorosulfite intermediate. Due to the improvement from the nucleophilic of the oxygen caused by S=O bond from thionyl chloride, the hydrogen atom of O-H bond gives up its electron and leaves the compound to connect with the leaving chloride ion in the first step; producing the hydrochloric acid. In the next stage, the graphene is suggested to be the electron donor temporarily, which provides an electron to forsake the SO_2 from the thionyl chloride compound and prepare a new chloride ion. This new chloride ion is attracted back to the benzyl on graphene as a nucleophile, because of the cutback from graphene. That finally forms benzyl chloride.

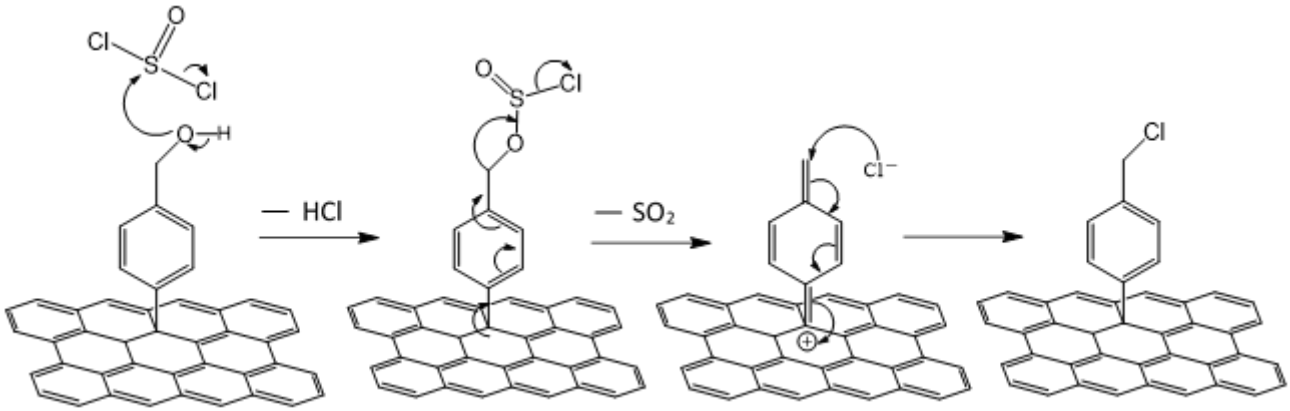

FIGURE 9: Possible mechanism for the benzyl chlorides formation, based on a similar conversion from an ether benzyl alcohol (Rodriguez and Priefer 2014).

2.4.3 Single-electron transfer living radical polymerization

For the enhancement of the association between graphene and other material, surface polymerization of graphene was studied to grow polymers brushes on the graphene sample. The graphene oxide has been reported successfully in polymerization using single-electron transfer living radical polymerization (SET-LRP), in which the covalent anchoring of bromine-containing initiator was used onto the surface of graphene oxide (Chen, Xiaoyi, Yuan, Yang, Hu, and Yang. 2011; Lligadas, Grama, and Percec 2017). Beside the SET-LRP method, the brushes can also be obtained by the original atom transfer radical polymerization (ATRP) (Zheng, Shen, and Zhai 2013) process, which is similar with SET-LRP. However, ATRP needs to be under some conditions, such as more time and metal catalyst for the reaction (Matyjaszewski 2012). While SET-LRP is more efficient and simpler since the reaction can be done in ambient environment and short time.

SET-LRP can be employed in a great variety of monomers and be tolerant for air and radical scavengers (Lligadas, Grama, and Percec 2017). The mechanism of SER-LRP is not entirely understood today, however, the mechanism proposed in Figure 10 is widely accepted (Levere, Martin, Nguyen, Leng, and Percec. 2013). The disproportionation of the copper(I) halide (CuX) generated by activation with pure copper (Cu^0), which is from wire or powder, is the crucial step in SET-LRP. Based on heterogeneous single-electron transfer (SET) mechanism, nascent Cu^0 activates the initiator and dominant chain, then starts the polymerization. During the polymerization, the propagating radical, $P_n^{\bullet}$, is formed by the activation step of Cu^0 with electro-acceptor alkyl halide initiator to generate CuX. The two possibility results for the radical-anion, which is concreted or stepwise, are depended on the substrate and the nature of the leaving group. The disproportionation of $Cu^{I}X/L$ into Cu^0 and $Cu^{II}X_2/L$ is the most important step, where reduction and oxidation happen instantaneously; $Cu^{II}X_2/L$ deactivates the propagating radical whereas Cu^0 activates the dormant species. This is facilitated by the presence of strong Cu(II)-binding ligands such as Me_6-TREN and PMDETA. This ligand solvent-mediated disproportionation of CuX prevents the undesirable bimolecular termination to accumulate the excess of CuX_2 deactivator and thereby reduces the risk of termination. Due to the responsibilities to series of "environmental conditions", including solvent polarity, the extent of disproportionation, nature of ligand and its concentration, the mechanism of SET-LRP can be deemed as a complex system, leading not fully understanding today (Levere et al. 2013).

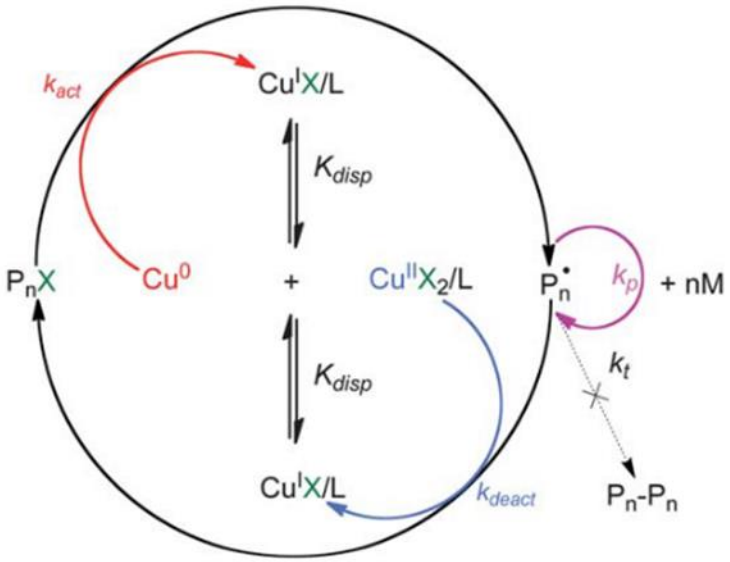

FIGURE 10: Proposed mechanism of SET-LRP (Levere et al. 2013)

In this project, the chlorine on functional graphene was used to be as the initiator for the polymerization process. Because the benzyl bromide could cause the over-polymerizing to the solution, leading to the

difficulty for controlling the process. While benzyl fluoride might could be tough to be activated for the polymerization, due to its strong bond with the benzyl group.

2.5 Fluorographene

Fluorographene (FG) is a new up-rising member in graphene family, which was reported as a stable graphene derivative by Sofo et al (Sofo, Chaudhari, and Barber 2007) and exploited more in later years (Robinson et al. 2010). FG possesses 2D layer structure and only have carbon fluorine bonds on the surface of graphene (Dubecký, Matúš, Otyepková, Lazar, Karlický, Petr, Čépe, Pvel Banáš, Zbořil, and Otyepka. 2015; Feng, Wei, Long, Feng, and Li. 2016; Karlický, Zbořil, and Otyepka 2012), leading to loss of delocalized electron on graphene surface; this is the reason fluorographene has a wide band gap, 7-8 eV, presenting as an insulator (Dubecký et al. 2015). Besides, FG possesses a high stability, thus, there a few solvents can be used to disperse FG. However, the dispersions of FG generally present in short-term stability (Zhu et al. 2013), limiting its manipulation and processing. FG can be prepared by fluorinating graphene (Robinson et al. 2010) or chemical/mechanical exfoliation of graphite fluoride (Dubecký et al. 2015; Zhu et al. 2013; Withers, Dubois, and Savchenko 2010). Due to these features, FG is used for insulating materials generally, besides, FG has been also undergone in various chemical reaction under ambient environment (Chronopoulos, Demetrios, Bakandritsos, Pykal, Zbořil, and Otyepka. 2017) to explore new graphene derivatives. In this project, FG is treated and used as the material for producing a high yield and selective functionalization of graphene by reacting with cyanine salt (Bakandritsos et al. 2017). The functional graphene from FG can be also used for making polymer brushes and composite material.

2.5.1 Cyanidation fluorographene

Due to the chemical inertness on the surface of graphene and graphene oxide, graphene derivatives are suggested to enhance the yield in functionalization of graphene. Because the graphene's surface and electronic properties is easier to be adjusted and manipulated with covalent derivatization graphene rather than immaculate graphene. A high functionalization degree on graphene was reported by Z. Radek and O. Michal et al (Bakandritsos et al. 2017), in which FG was treated with nitrile group (also known as cyano group), -C≡N or -CN, toward a broad scale. From this, the project got inspired to work on cyanographene.

Understanding the properties of chemicals is the key for predicting and controlling the reactions and direction for the goal of the project, thus, the FG characters in the reaction should be acknowledged. The supreme factor of FG is the high bond dissociation energy of C-F bond with 108-130 kcal/mol (Dubecký et al. 2015; Matochová et al. 2018), hence FG is an unreactive material mostly (Lemal 2004); consequently, direct cleavage C-F bond reaction is disfavored. However, there some methods and procedures have been studied and published about defluorination FG, which is based on the thermal stability of FG. In a report by O. Michal et al (Barès et al. 2019) in 2019, defluorinated FG was prepared by a high temperature, at 550°C, and sonochemistry, then the product could be ready for forward steps. Nevertheless, beside physical method for detaching C-F bonds, a bimolecular nucleophilic substitution reaction mechanism (S_N2) was also proposed, where simultaneous formation between carbon and a nucleophilic bond was used to cleave the C-F bonds and replace a new nucleophile at the leaving fluoride atom position as the same time (Dubecký et al. 2015). Feasible pathways for FG defluorination were demonstrated recently (Medveď et al. 2018), in which that reaction happens simultaneously with substitution and pointed the role of solvent. However, despite many reports in this field, there no conclusive mechanism of FG reactivity has been accomplished.

There are two types of nucleophilic (Nu) species are used recently, namely hydroxide (OH-) and cyano (CN-). They have been reported to successfully react with FG (Bakandritsos et al. 2017). Relying on theoretical calculation of the S_N2 reaction of FG (Matochová et al. 2018), the nucleophiles reaction with FG cannot be elucidated. However, the reaction could be commenced with single electron transfer (SET) from a nucleophile to FG, suggested by Lai et al (Lai et al. 2017), where a radical site on a carbon atom was created after the C-F bond gets ruptured by Nu- attack, see in Figure 11. Due to the negative charge of Nu species, the FG receives a negative charge. Then, the "next door" C-F bonds are more susceptible for heterolytic cleavage, giving up fluoride ions to the environment; particularly, the C-F at ortho position was favored to get triggered in the breaking chain for all cases. After the F^- detachment, a newborn radical center is made and attacked by another Nu, and the process keep going on. This repetition causes functionalization on graphene sheets and also releases fluorine atoms to restore the delocalized electrons system on graphene again, reviving conductivity on graphene.

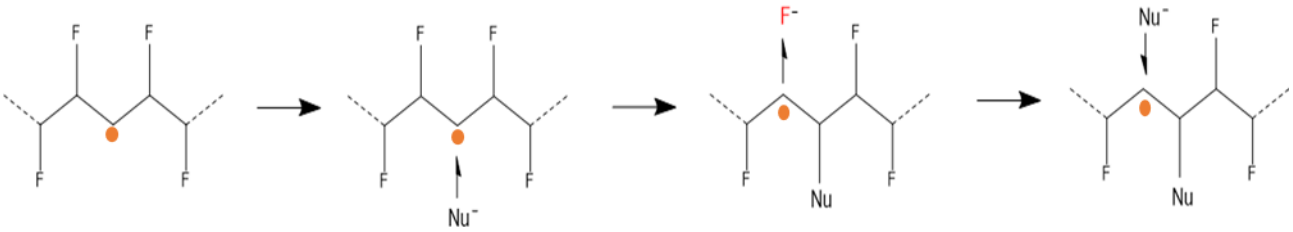

FIGURE 11: Suggestion of Nucleophilic attack on FG and CF bonds rupture (Matochová et al. 2018).

2.5.2 Amine conversion from cyanographene

Because of the limit reactions from nitrile functional group in cyanographene with other chemicals, conversion –CN group to other activating functional groups such as acid (–COOH), hydroxide (-OH) or amine ($–CH_2NH_2$) is suggested and studied; because those active groups can connect easily with other compounds to build network systems. The conversion of $COOH^-$ from CN^- on fluorographene has been reported successfully by (Bakandritsos et al. 2017), besides, the acid functional groups on graphene can be found in many literatures from graphene oxide. Due to the basic properties of amine, this moiety is proposed to replace the cyano group on graphene. Another direction of using functional graphene could be opened via this amine functional group, which can be used to react with many compounds/polymers possessing acid group or with active oxygen from various compounds such as ketone, acryl, aldehyde, epoxy, isocyanate (Jaker and Baile 1957).

Lithium aluminum hydride (LAH), $LiAlH_4$, is employed for the nitrile to amine conversion reaction. This reaction is well-known as hydrogen reduction for amine, introduced in many synthesis organic chemistry textbooks. The LAH is usually used to convert from nitrile to amine at the according position for many compounds such as alkene, benzene or cyclopentane. Thus, LAH is promising to convert nitrile on graphene to amine group and the reaction is based on the very basic of reduction of nitrile with LAH, referred to the first report of a C-CN bond cleavage (Mattalia, Samat, and Chanon 1991).

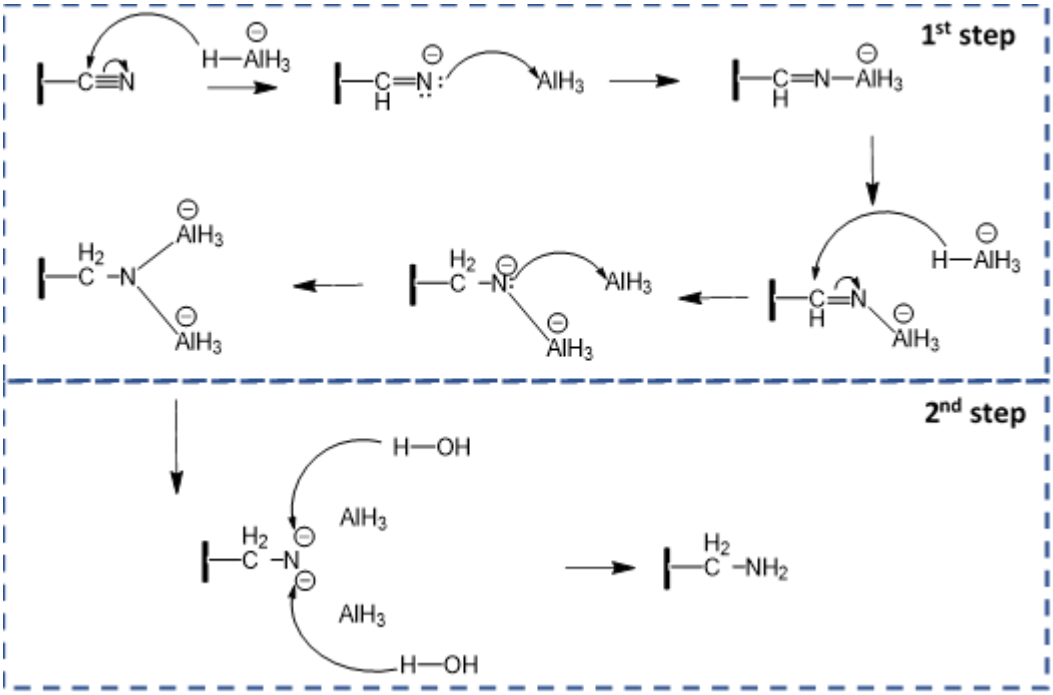

FIGURE 12: Proposed mechanism of amine conversion on graphene, based on mechanism nitrile to 1° amine (Steven Farmer 2019)

By surveying the reactions of amine conversion from various compounds, it is noticeable that the hydrogen reduction is happened at only nitrile group without any impact or influence from the main compound, on which the nitrile is attached. Therefore, a proposed mechanism of the reaction on the graphene is depicted in the Figure 12. There are two steps in the mechanism, first step is double addition of hydride and second step is aqueous workup. In the first stage, the hydrogen from LAH attacks to the polarized carbon of nitrile at the π bond of –CN via nucleophilic addition. An intermediate is formed after the nucleophilic addition and which is complexed with AlH_3- instantly. This sequence is repeated with another LAH to break the second π bond in –CN, then a complex between CN^- and two AlH_3 is made and the sequence is stopped, ending the first step. Moving on the second step, the hydrogen of water is attracted by the nucleophilic nitrogen from the –CN and replaces the AlH_3, resulting the amine group formation. The side products from the reaction includes lithium hydroxide (LiOH), aluminum hydroxide ($Al(OH)_3$) and hydrogen gas (H_2).

3 EXPERIMENTAL

There are two main experiments, namely graphene exfoliation and fluorographene, which are studied and developed extensively in this project. The detail procedures of both topics will be shown vividly. Besides, some important choices of chemical during the experiment will be explained explicitly.

3.1 Graphene exfoliation

There were three experiments in this topic which was aiming to build brushes on the graphene from the raw material, graphite. The approach of brushes graphene is followed order from producing functional graphene, then chlorination hydroxide group and lastly building brushes.

3.1.1 Procedure of electrolysis

The apparatus is shown in Figure 13, where the cathodes were two platinum (Pt) plates with size 9 x 3 cm and a highly oriented pyrolytic graphite (HOPG) (99.8%, Alfa Aesar), which was measured approximately with the size of the Pt plates, was used as the anode. The mass of graphite was measured to calculate the yield in the end. The electrolyte was made from 100 ml of 0.1 M sulfuric acid. The functional group, 0.05 g of benzyl alcohol diazonium salt, was added into the electrolyte. The reason using this be benzyl alcohol diazonium salts was to utilize the single carbon from alcohol group, which is promoted by the active of the benzene ring; and later for the Cl- ion in polymerization step is also supported from the benzyl. The gaps between cathodes and anode were around 2 cm. A power source with DC of 10 V was employed to initiate the electrolysis process, the reaction duration was circa 1 hour. After the reaction, both cathodes and anode were rinsed with demineralized water to collect all the product on the surface of electrodes. The remained graphite, which was not emerged into the electrolyte, was dried, in oven with 100°C in 24h, and weighted to find out the amount of participated graphite in the reaction. The functional graphene was called EG-OH as a short name in this project.

FIGURE 13: Apparatus of electrolysis: the anode is the red clip, and in the middle. The two cathodes are the black clips in the both ends of the sides.

A 0.45 µm nylon membrane was employed as the filter for the filtration. The bulk in electrolyte was filtrated and rinsed with acetone nitrile, which was used to wash off the excess salt in the bulk, and later with water. The product, then, was dissolved back into N-Methyl-2-pyrrolidone (NMP) with the support of sonication tip (BRANSON, frequency 50/60 kHz, power 550 W), which was set 175 W as the effective power within 10 minutes. After that, the dispersed graphene was transferred to centrifugation step. The first time of centrifugation was used with 1000 rmp in 10 minutes to remove the leftover graphite (big part) which was not exfoliated completely in electrolysis process. The fine graphene was collected with centrifugation with 4000 rmp in 2 hours. Water was also employed to clean NMP by the same centrifugation with 4000 rmp and in more 2 hours. The collected graphene could be either dissolved back into water for storage by using freeze drying method or used forward for the next steps. After the freeze-drying process, the product looked like aerogel, see in Figure 14.

FIGURE 14: Graphene products from exfoliation method

3.1.2 Chlorination

100 mg of the functional graphene was dispersed in 100 ml of dry toluene. 1 ml of Thionyl Chloride was added in the solution. The reaction was carried out in nitrogen atmosphere and room temperature and was left for reacting in different duration time, 24 hours to 72 hours. After the reaction, the chlorinated functional graphene (EG-Cl) was collected by filtration and rinsed with different solvent, following the order, hexane, water and acetone; by which the excess thionyl chlorine was washed away by hexane, the water was aimed to clean hexane. Due to the hydrophobic property of graphene, some of product were stuck on the wall of funnel, hence acetone was employed to gather entire graphene on the filter. The EG-Cl was dissolved back in water and stored via freeze-drying process.

3.1.3 Polymerization

6 mg of chlorinated functional graphene (EG-Cl) was dispersed in mix solvent, made of 12 ml of water and 6 ml of methanol. 220 µl of N,N,N',N",N'"-Pentamethyldiethylenetriamine (PM DETA) was added in the solution. The solution was also purged by argon (Ar) gas to ensure the reaction occurring in inert environment. Because the nascent copper (Cu^0) can be active with oxygen to produce copper oxide which could stop the SET-LRP process. 12 ml of monomer (Hydroxyethyl)methacrylate, called as HEMA, was introduced in the solution. Copper wire was used as the copper source for the reaction, which was wrapped around a magnetic bar, dubbed as copper magnet. The copper magnet was the key of reaction commencement; hence it was dropped in the solution at the last. The reaction was stirred in Ar environment, maintaining the inert condition, within 1 hour. The product was filtrated and rinsed with water and ethanol. The polymerized graphene (EG-P), then, was dispersed in water to process the freeze-drying method for collection and storage.

3.2 Fluorographene

There were two experiments carried out in this section, including cyanidation fluorographene and amine conversion. The goal of the experiments was about to transform fluorographene to an employable functional graphene, helping the project.

3.2.1 Cyanidation fluorographene

The procedure was based on a paper from (Bakandritsos et al. 2017) and it was changed a few factors, because of facilities availability. There are two parts in the procedure, including sonication step and cyanide salt reaction. In sonication stage, 0.06 g of graphite monofluoride was dispersed in 60 ml DMF in two different procedure by two different sonication types, namely sonication tip and sonication bath, within specific times which was relied on the effective power used in each sonication. To differentiate two procedures, they were called as the long-term process (L), which was run by sonication bath, and short-term process (S), in which the sonication tip was employed, and the samples from these processes were named FG-L and FG-S, respectively. The reasons for the names was about the duration of the sonication; the sonication bath used longer time to disperse FG, due to its low power output, while the tip one set at high effective power was used in short time. Due to the low power (BRANSONIC, 90 W, 50-60 Hz) of the sonication bath, the time for reaction was up to 7 hours, and during the sonication, the solution was under nitrogen atmosphere. While the tip sonication (550 W, 50/60 Hz) was used 324.5 W within 30 minutes in ambient condition.

After the sonication, FG was treated with 0.52 g of potassium cyanine (KCN), according to mole ratio 1:4 between FG and cyanine, in a round flask. The reaction was heated at 130°C and stirred 500 rpm under a condenser and in oxygen free condition during various time, from 22 to 25 hours. The solution was cooled down at room temperature before treating with a massive washing step. The FG was transferred to centrifugation for washing step with different solvents, namely Dimethylformamide (DMF), Dichloride methane (DCM), acetone, ethanol. After that, 80°C of DMF and water were used for the last washing stage. The centrifugation was adjusted at 4000 rpm and ran in 30 minutes during the washing process. The conductivity of the FG was checked to ensure there was no KCN remained; if the conductivity was higher than 200 µS/cm, the FG had to be washed more. The main idea in this washing step is to eliminate the excess KCN salt, which is a toxic compound. After the washing, FG size was classified with centrifugated at 1000 rpm in 10 minutes, in which the big part assumed as graphite was discarded. Then, the product from the process, called as FG-CN was stored by freeze-drying technique.

In the reaction with cyanide salt (all samples were run with short-term process in sonication step), there also different ways were performed. Tetrabutylammonium cyanine (TBA) was replaced for KCN and the ratio moles between cyanine and FG was remained, and the sampled was called FG-TBA. Another procedure, which employed mixed solvent, containing DMF and water with the ratio 6:1 (v/v); this mix solvent was supposed to maintain cyanide salt dissolving during the reaction; the sample was named as

FG-wet. In excess-cyanine removal step, the washing step with centrifugation using diverse solvents was swapped with filtration and rinse with acetone and water; it is worth to use an extra of water in this step. Particularly, in filtration step, a 0.45 µm filter was used and acetone was firstly used to collect all FG-CN in the flask, then water was introduced to clean the cyanide salts. The FG-CN from filter was collected by dissolving back in DMF and using the centrifugation to wash off DMF with water. Then the FG could be stored by freeze-drying method after the centrifugation step.

3.2.2 Amine conversion

12 mg of cyanided FG (FG-CN), which was from FG-wet, was dispersed in 25 ml of dry toluene in a 50 ml round flask. The flask was, then, placed in an ice bath before adding 10 mg of $LiAlH_4$ (LAH). For explosion prevention, all equipment contacting with chemicals was prepared as water free as possible and the temperature was kept low from 0-5°C during the beginning of the reaction. The reaction was stirred during 25h and under nitrogen atmosphere. In the quenching stage (or called as hydrolysis step), 4 ml of chloric acid 1 M was added, and the reaction was still stirred and under the inert gas. The reaction was shown quickly and in short time aggregation and precipitation were occurred in whole the solution. Then the solution was filtrated and rinsed with water and the product on the filter was dispersed back in to DMF. Storing and collecting the converted FG-CN (FG-NH_2) could be done by freeze-drying method.

4 RESULT AND DISCUSSION

All the samples from both graphene exfoliation and fluorographene were characterized mainly in Raman and XPS. The samples were prepared and deposited on substrates (SiO_2), which is described in appendix I, and filtrated through a nylon membrane for Raman and XPS analyses, respectively. In Raman analysis, samples on SiO_2 plates give spectra with little noise, leading to clear and vivid peaks and accurate analysis. While in XPS, the filters were left in an oven at 100°C for at least 24 hours, before making the analyses with the machine. Because the leftover solvents (water, NMP or DMF) on the filter need to be evaporated completely out of the samples, otherwise analyses could be influenced and distorted.

4.1 Graphene exfoliation

The product collected in the end of the exfoliation process could achieve approximately 50% yield (w/w), compared with the used graphite. The sample was compared with a blank pristine graphene which was made by the same setup electrolysis without diazonium salt. The comparison, in Table 1, showed explicitly the dissimilar intensity ratio D/G from two samples, functional and pristine (blank) graphene.

TABLE 1: Comparison ID/IG ratio between functional and pristine graphene

Sample	I_D/I_G ratio	G position (cm^{-1})
Functional graphene	1.1 ± 0.2	1588 ± 1
Blank graphene	0.5 ± 0.1	1583 ± 0

The samples analyzed by Raman, in Figure 15, showed a high D peak, evidencing for the appearance of functional groups on graphene. Basing on the results from I_D/I_G ratio and spectra images, the graphene was changed from sp^2 hybridized carbons to sp^3 hybridized, which was observed in D peak. Moreover, the 2D peak in functional graphene indicated that there was still structure of graphene in the sample and the functionalization occurred partially on the graphene. This was also the goal for the functionalization on graphene, since the properties of graphene was remained and could be employed, while the functional group on graphene supported to affiliate graphene with other materials. Due to the impact of the functional group on graphene, the G band was shifted from 1583 to 1585 cm^-. There was also a presence of D' peak, which was detected as a shoulder of G peak.

By using the prementioned equation (1), the quantification of defects of functional graphene sample was calculated. The I_D/I_G ratio from table 1 is inserted to the equation (1) to find out the distance among defects (L_D) and the defect density (σ), the detail of calculation is shown in appendix II: Raman Calculation. According to the result of the calculation, there are about 442 carbon atoms per a defect in the functional graphene sample. However, it is cautionary that the Raman cannot distinguish which types of defect on graphene sheet, therefore, the defects could include possibly both functional group and oxygen, which was caused inevitably by oxidation on graphene from exfoliation step. This explains the 1050 carbon atoms per a defect on blank graphene sample (calculated from the intensity ratio), which is from grain boundaries, vacancies, edges, hetero structures and interstitial impurities in graphene (Haldar and Sanyal 2016). Thus, the calculated defect densities could not show the exact number of defects provided from functional groups.

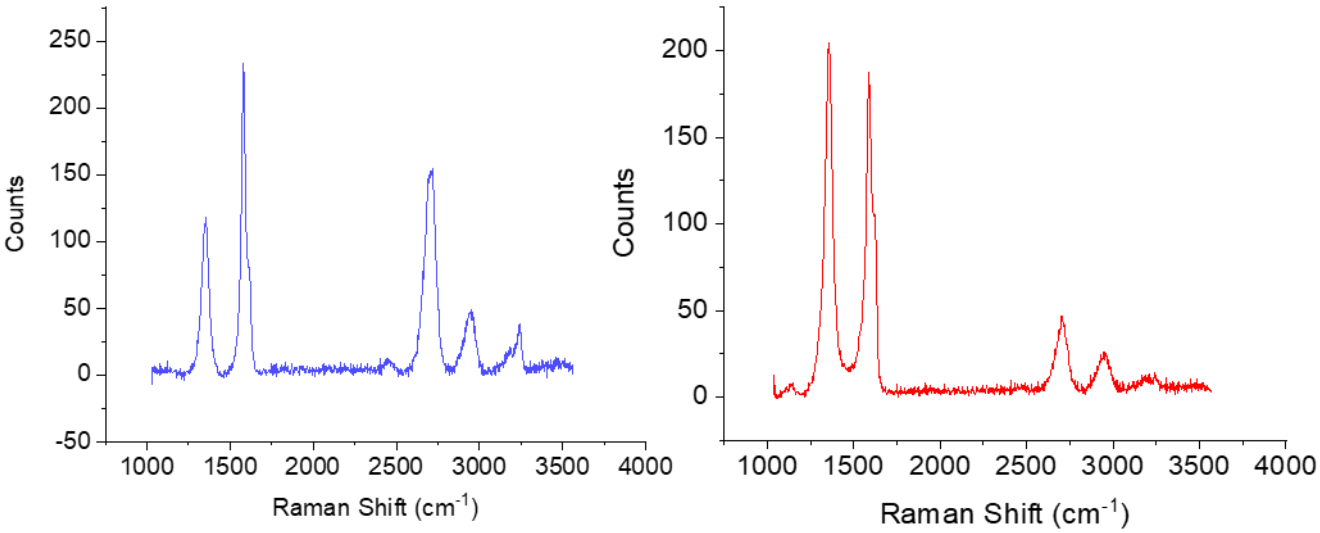

FIGURE 15: Raman spectra of pristine (blue line/left) and functionalized graphene (red line/right).

Basing on the equation (2) and (3), the number of graphene layers could be estimated from Raman analysis. In the functional graphene sample, the position of 2D peak is around 2718 cm^-, hence the intensity of I' should be from the peak around 2688 cm^-. While the 2D peak of HOPG sample is 2727 cm^-, then the I' could be found from the peak at 2697 cm^-. By introducing the intensity peaks from both functional graphene and graphite in equation (2), the M is calculated, then, replacing the M value into equation (3), the number of layers is figured out about 6 to 7 layers.

By using AFM measurement with taping mode, the number of graphene layers could be confirmed by estimating from the thickness of the flake on the substrate. The sample for AFM was prepared the same

way for Raman measurement; the graphene flask was on top of SiO substrate. The average thickness of the flask ranged around 10.5 ± 1.2 nm; there some flasks with 4.2 ± 0.5 nm in height, and the length of the flasks was about 5 µm. In Figure 16, there are some white lines crossing on the graphene sheet, which is supposed to be the wrinkles of the flakes, since the graphene somehow got folded instead of spreading; this might be caused during the sample preparation. This also could be a problem for getting a proper thickness of the flake. The thickness from a single graphene layer is summarized from various AFM method, resulting the range from 0.4 to 1.7 nm (Stapleton et al. 2016). The thickness from a single layer is essentially considered about the remained solvent compounds and defects from both functional group and interstitial impurities between graphene layers. Therefore, the range of number of graphene layers from the sample is from either 10 to 26 layers or 2 to 6 layers, according to the range of one single graphene layer from the AFM measurement.

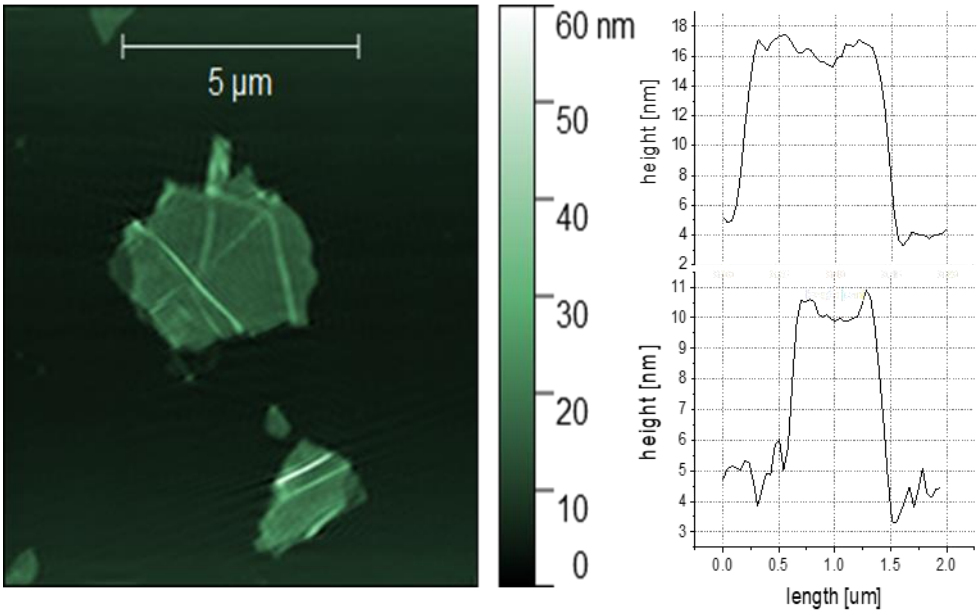

FIGURE 16: AFM graphene image using contact mode (left) and profiles from different cross section on the flakes (right)

4.1.1 Chlorination

Chlorination reaction only attacked on the OH^- on the functional group, leading to no influence on the graphene sheet and no new defect creation. Therefore, only XPS was applied to check out the achievement possibility of chlorination process. The Table 2 shows that there was no different from chlorination for functional graphene with 24h and 72h, meaning either that is the maximum the chlorine replacement

for hydroxide group or that is the total number of functional groups on graphene, when chlorine has exchanged for all OH- group.

TABLE 2: XPS analyses of Chlorination of functional graphene in XPS survey spectrum. Where C1s, Cl 2p, N1s and O1s are the percent of carbon, chlorine, nitrogen and oxygen in the sample, respectively.

Samples	**Carbon C 1s %**	**Chlorine Cl 2p %**	**Nitrogen N 1s %**	**Oxygen O 1s %**
Pristine graphene	95.67	0	0	4.33
G-OH	85.54	0	1.74	12.04
EG-Cl in 24h	88.97	0.1	0.55	10.39
EG-Cl in 72h	90.01	0.1	0.41	9.50

The number of chlorine atoms, relied on the results, could predict the amount of polymer brushes which could be connected to the graphene sheet via the exchanged chlorine atoms on graphene. The number of chlorine atoms detected is equal with the number of chlorinated functional group, and each functional group have 7 carbon atoms, because of the benzene ring and methyl. Therefore, the potential polymer brushes could be calculated in the equation 5 and that are about 889 carbons per brush in 24h and 899 carbons per brush in 72h.

$$\frac{C}{Cl} = \frac{C1s\ \% - 7\ x\ Cl2p\ \%}{Cl\ 2p\ \%} \qquad (5)$$

4.1.2 Polymerization

The same effect with chlorination reaction, polymerization process did not influence to the graphene sheet, leading to using XPS for the analysis. Because of the similar for both chlorination reactions, one of samples could be used for representative for all. In the appendix I table, the polymerization result displayed the absence of chlorine in the survey spectrum on the sample; however, chlorine could be traced by XPS with a very tiny amount, meaning that the occurrence of the polymerization process was confirmed via this impact. The small amount traced chlorines could not be expressed, caused possibly by the long chain of the attached polymer brush, in which, the amount of total carbon and oxygen was enormous by far, compared with the chlorine quantity. The rise of oxygen percent in the sample was observed and improved, due to the C-O and C=O bonds at band around 286.7 eV and 288.98 eV, respectively, from HEMA. In the high-resolution spectra, see in Graph 1 in appendix III, the developments

of peaks C-O and C=O are presented lucidly, and in Table 3, the C=O area of EG-P was increased significantly, compared with EG-Cl sample's.

TABLE 3: The comparison on % area of bonds in XPS of polymerization in high-resolution XPS scan spectra.

Samples	**C=C**	**C-O**	**C=O**
EG-Cl	41.29	22.22	3.78
Polymerization	27.78	21.62	18.73

4.2 Fluorographene

Fluorographene (FG) is recently used to enhance the strength for insulating materials, due to its properties. In recent years, the FG is undergone with many researches focusing mainly on the insulation, hydrophobicity, strength and thermal stability for material. However, producing functional graphene from FG is a new and promising pathway of graphene derivatives from this FG field. By using substitution reaction for FG, a high yield of functional groups assembled on graphene and bringing conductivity back for graphene, simultaneously. In this project, the FG is functionalized by nitrile group and later converted to amine group in the next level. The FG samples were analyzed and identified with XPS, where the samples all were prepared as free-standing films on nylon membranes.

4.2.1 Cyanidation fluorographene

The pristine powder FG was firstly analyzed as the control sample for whole the FG experiments, comparing FG samples treated with cyanine salts. During the experiments, in both long-term process (FG-L) and short-term process (FG-S), there was always a large amount of solid precipitated in the bottom of flasks. Thus, coming to the suggestion that the cyanine salt was not dissolved completely in solution. Therefore, a wet solvent in which water was mixed with DMF was used to help dissolving and prolonging the cyanine presence in the solution; the sample for the reaction called FG-wet. In another reaction, Tetrabutylammonium cyanine (TBA) was used for the reaction without water, because TBA can easily give up its cyano group in solution and the samples of this reaction named FG-TBA.

The cyanide groups were also chosen, because they were used to not only remove fluorine but also to replace fluorine and play as a functional group on graphene sheet as S_N2 reaction, which is more concerned. In the Table 4, the values of nitrogen (N%), fluorine (F%) and carbon (C%) of all FG samples, comprising pristine FG, FG-S, FG-L, FG-wet and FG-TBA in XPS survey spectrum, was compared to perceive the differences.

TABLE 4: Comparison of elements in different FG samples in XPS survey spectrum

Samples	**C%**	**F%**	**N%**
Pristine FG	47.78	52.22	0
FG-S	73.11	22.49	1.8
FG-L	66.32	30.61	1.48
FG-TBA	84.48	9.86	2.24
FG-wet	71.9	23.64	1.41

The structure of fluorographene is covered full of C-F bonds(Yang Yang et al. 2013) even after the sonication treatment from graphite fluoride, proved by the absence of conductivity and super hydrophobic characters on the FG samples. The FG-S and FG-wet, which have the same sonication treatment (mentioned in experimental section 3.2.1), could achieve more than a half defluorination in total of fluorine atoms (F), while in FG-L just only treated about 20% of F on FG. This means the short-term process is more effective than the long-term one, implying the sonication power could improve the success in defluorination; in which the more power is used to the sonication step and the better defluorination is. However, the sonication type also needs to be taken in to account. Because the sonication tip was reported as the advanced sonication method for exfoliating graphene, compared with bath type sonicator(Amiri et al. 2018). From the dissimilar results of defluorination from FG-S and FG-L samples in sonication step, the quality of FG-CN could be deceived by exfoliation with sonication.

One of the reasonable suggestions for this difference is about graphene layers of FG, because the initial material used in the experiment is graphite monofluoride. Hence after the sonication stage, the fluorographene is produced, presenting various layers flakes, meaning there are some flakes consist of few layers and others have many layers, see in Figure 17. The samples in FG-S is supposed to have fewer layer than the one in FG-L, due to the type of sonicator. Based on the number of graphene layers in FG flakes, the graphene layers are insinuated like the “shields”; the less graphene layers of the flake are, the weaker the “shield” becomes. Thus, the CN^- from the cyanide salts could expectedly attack easier to the

FG with less layers rather than the thick FG with multilayer of graphene, hence the fluorine atoms could be influenced from both sides by the salt.

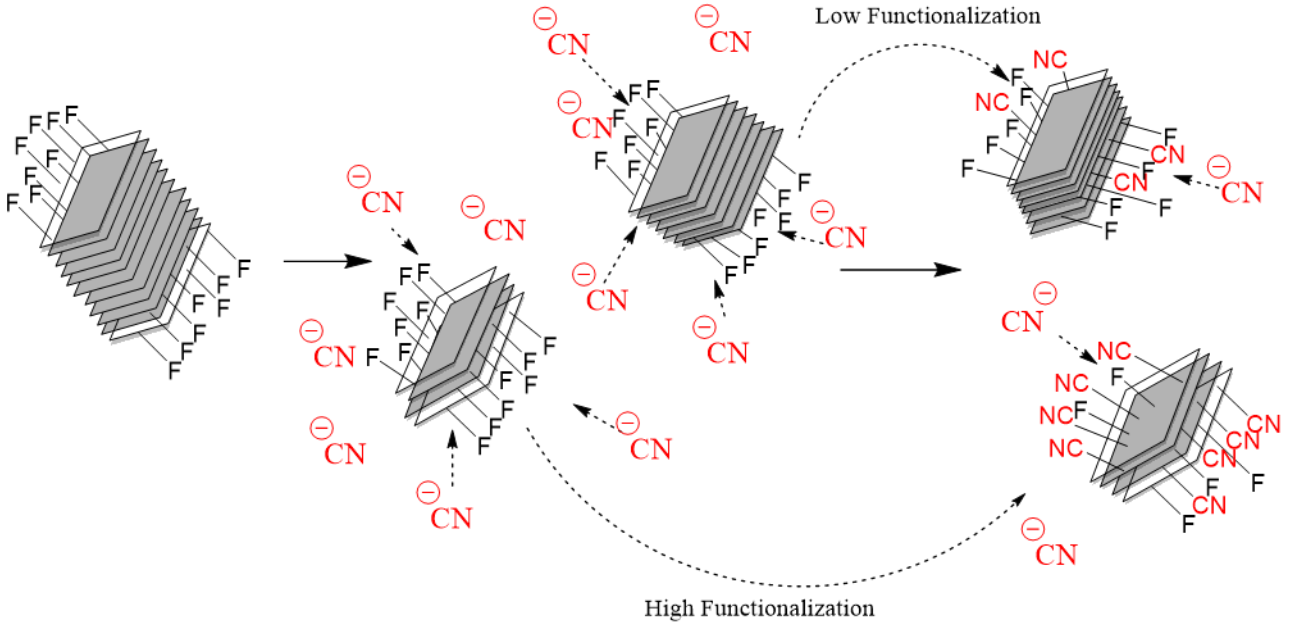

FIGURE 17: Proposed prediction of fluorographene treated in sonochemistry influencing to S_N2 reaction. Where the less the number of graphene layer is, the more efficient the S_N2 could obtain.

Based on the XPS measurement, the FG was successfully treated with two cyanide salts, namely KCN and TBA, which was proved by restoring the conductivity of graphene sheet. The amount of fluorine in treated samples is apparently dropped significantly with TBA salt, which is more than 81% loss of F in the content. The massive fluorine reduction from FG-TBA could be proposed the impact from CN^- presence in the solution, where CN^- of TBA salt could be released easily; the moisture, even, could dissolve the salt. While KCN requires a certain amount of water to be dissolved; the solubility of KCN in water was estimated with ratio 1:2 (g/ml). Therefore, the FG-CN sample treated with TBA got more attacked from CN^-, resulting losing more fluorine atom. Nevertheless, the solid part found in the end of the reactions, regardless of types of salt used, could be either the reactants, including insoluble cyanide salt and FG aggregation(which might be caused by the low Zeta potential (about -30 mV) (Zhu et al. 2013; Bakandritsos et al. 2017), or side products, which is unknown, or both reactants and side products. Noticeably, the solid part could be mainly washed off by water, neither DMF nor acetone, hence that is supposed to be ion compounds.

In nitrogen (N) comparison, the FG-TBA again is the highest amount, compared with others, however the differences are narrow. All the samples reacted with KCN shows similar amount of N detected, while

the one treated with TBA salt was higher, thus, that confirms the importance of CN^- in the solution. However, there an odd factor is necessary considered that is the vast gap between the number of fluorine atoms detached and the amount of nitrogen, indicating cyanide group, replaced on the graphene. Because according to the S_N2 reaction theory, the reaction should be carried out with ratio 1:1 between F^- and CN^-, however, in the analyses, there a few CN^- successfully exchange with F^-. The question for this is more about only the defluorination possibility, rather than the way of cyanide replacement, because of the obvious occurrence of the substitution reaction (Dubecký et al. 2015; Medveď et al. 2018; Lai et al. 2017) for that replacement.

Rewinding back to the theory of cyanidation FG (Matochová et al. 2018), a potential pathway of defluorination is illustrated in Figure 11. The fluorine atoms on the covered surface could be triggered to leave the graphene sheet and form a radical on the surface. That radical is supposed to react with a CN^- in solution to render a C-CN bond on graphene. That C-CN bond effects to the orthro carbon on the benzene ring, by which the "next door" F^- is forced to leave and create a new radical, then the sequence is continued.

However, if there many fluorine atoms get attacked to leave at the commence, meaning to lots of the CN^- replacing at the same time. Thus, in the next step of the pathway, after the fluorine abandonment, two radicals supplied from two next door carbons could arrive to a same carbon. This carbon might both refuse CN^- localization and reinstate the delocalized electrons of benzene ring, which helps to release other F^- from other carbons on the ring. Furthermore, another activation of CN^- on graphene is the termination each other of CN^-, when they locate side by side and these CN groups also could push other fluoride atom neighbors out of graphene, see in Figure 18. When both CN^- and F^- are absent, the delocalized electron is established back on the benzene and stops the immigration of nucleophiles. This might explain about the return of conductivity of graphene from FG. In addition, the different time in reaction does not influence much to the results of FG treatment in the range from 22 h to 25 h. However, if the time is about 1h or 6h, the functionalization yield might be increased.

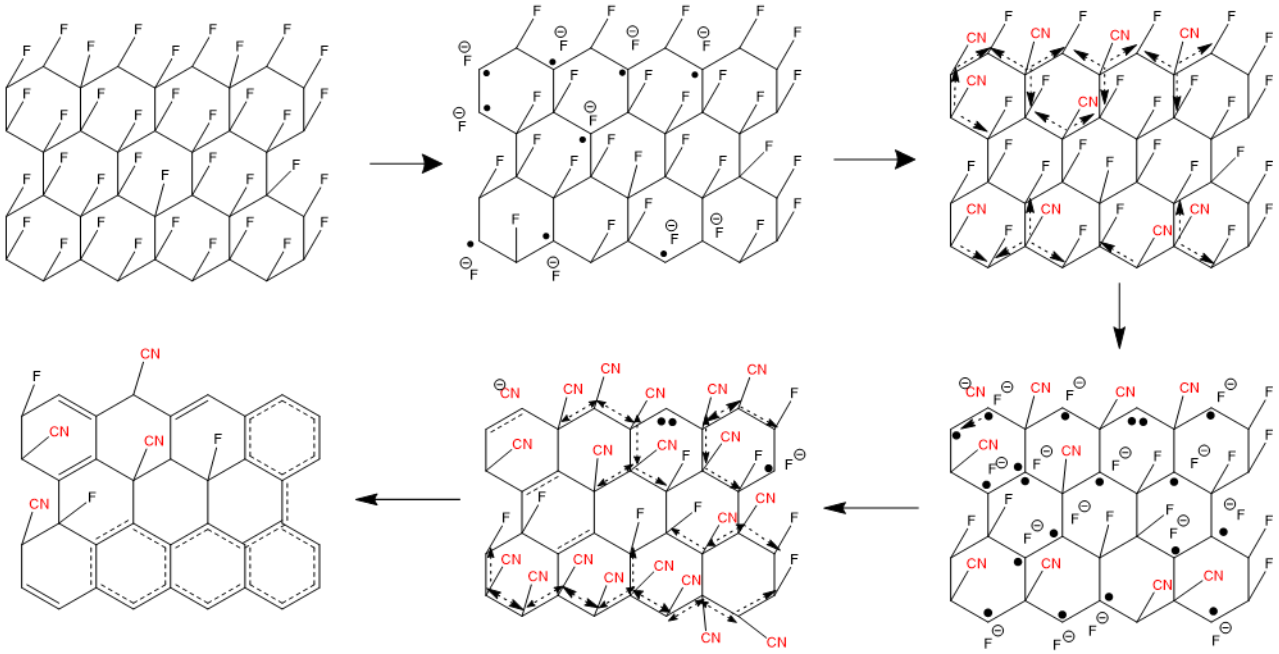

FIGURE 18: Mechanism suggestion for S_N2 reaction between fluorographene and cyanine salt.

The change of the percent of carbon from cyanidation samples could again enhances the success of functionalizing CN^- on the graphene sheet. It is undoubtedly that the number of functional groups on graphene is the most important for the aim of the process. Thus, the number of CN^- groups on graphene could be calculated by equation in appendix II, which is followed the same way for finding the amount of Cl^- on graphene in chlorination. There are roughly 40 to 50 carbons per one the functional group, CN^-, for FG treated with KCN salt. While the FG-CN reacted with TBA could achieve more functional group on the graphene sheet, which is 36.7 carbons per one functional group, see in Table 5.

TABLE 5: Comparison of functional group density on FG among samples

Sample	**FG-S**	**FG-L**	**FG-wet**	**FG-TBA**
number of carbons per CN^-	39.6	43.81	50	36.7

Considering about the fluoride reduction, in the pristine FG, the ratio between C/F is about 1:1. After the process, the amount of fluorine atoms is dropped and the ratio C/F is about 2.8:1, while the TBA salt could reduce the fluorine with ratio C/F about 8.6:1. Although the decrease of F quantity is showed, that does not show the conductivity restoration on graphene sheet via XPS survey, because they might be the exchange between F^- and CN^- on graphene. The evidence of the return of the conductivity could be analyzed in high-resolution spectra, see in figures Graph 3, Graph 4, Graph 5 and Graph 6 in appendix

III, where the C=C area, located around 284.5 eV, raises largely and clearly in all treated samples, compared with the control sample, see in Graph 2 in appendix III. In contrary, the C-F bond declines remarkably, due to the loss of fluorine on FG at binding energy 289.2eV and the appearance of CN bond is detected at 288 eV.

However, the aim of using functional groups on graphene is to enhance the connection between graphene sheets and commercial polymers in composite materials. Thus, the properties of graphene, strength and conductivity, are essentially taken into account of functionalization. If the functional groups cover completely the graphene sheet, the conductivity of graphene will be reduced significantly or even lost. Therefore, the high yield of functionalization should have a compromise with the quality with graphene capacity in the composite material. Nevertheless, controlling the number of functional groups on graphene is strong recommended, hence, understanding the mechanism behind the functionalization on FG should be approached, in order to manipulate the yield of functionalization for the desire results in composite material.

4.2.2 Amine conversion

Due to the first time of the experiment of amine conversion from cyanographene in the project, the XPS measurement was used to identify all the elements presenting in the sample. In the XPS survey spectrum, see in Table 6, it is worth to notice that the aluminum presence in the sample. Because the aluminum should be reduced complete in the hydrolysis step, resulting the unaccomplished hydrolysis reaction; even an extreme chloric acid solution added, compared with the amount of LAH and cyanographene. This might be caused by impediment of aggregation and precipitation in hydrolysis reaction, by which the compounds quickly gathered to each other and lessened the reaction area of the unreacted compounds, resulting to the low yield in hydrolysis. The aggregation and precipitation were mainly formed by lithium chloride (LiCl) which is insoluble in toluene and aluminum chloride is also very hard to dissolved in toluene (Pruntsev, Arkhipov, and Mikheeva 1972). Besides, the huge amount of LiCl could be produced from the excess amount of LAH at the beginning; the LAH is neither dissolved well in toluene (V. I. Mikheeva, S. M. Arkhipov 1972). Therefore, the hydrolysis was not performed completely when the clusters developing.

TABLE 6: Elements presenting in the sample from anime conversion, analyzed by XPS survey spectrum

Elements	**Carbon (C1s)**	**Oxygen (O1s)**	**Nitrogen (N1s)**	**Fluorine (F1s)**	**Aluminum (Al2p)**
Percentage of Area (%)	59.64	12.97	1.33	24.59	1.47

The reason toluene employed in the reaction is because the graphene can easily be dispersed well in the solvent, giving more area for the reaction between CN and $LiAlH_4$. Besides, unlike THF used in the literature (Mattalia, Samat, and Chanon 1991), toluene does not polymerize during the reaction, reducing risk of impurities in the sample. The solution for hydrolysis reaction improvement is suggested to add a large amount of water or chloric acid solution to the reaction in order to dissolve the salts in solution and keep the hydrolysis reaction continuing. The amount of the suggesting addition water might be one fourth amount of toluene volume. Because there 4 ml of the acid was used in 25 ml of toluene and the hydrolysis reaction was approximately carried out a halfway, based on the ratio of Al/N about 1.1 in the sample (derived from Table 6), while the ratio Al/N before the hydrolysis step should be 2 (see mechanism in Figure 12). Furthermore, the pH of the acid should be probed due to the agglomeration of graphene in water, caused by low Zeta potential (He. 2017).

If the extra water in the suggestion for hydrolysis worked, it would be excellent choice to use chloric acid instead of water, as the article (Mattalia, Samat, and Chanon 1991). Because the $Al(OH)_3$, one of side products from the hydrolysis with water, is insoluble in water, which is not able to be wash off in filtration step. Besides, it is apparently that the LiOH and $Al(OH)_3$ cannot be dissolved in toluene because toluene is a nonpolar solvent. Thus, the side products from chloric acid solution, including lithium chloride (LiCl) and aluminum chloride ($AlCl_3$), can be dissolved well in water, refraining precipitation and aggregation in the solution, resulting to the continuation of hydrolysis reaction.

In the high-resolution XPS spectra in N1s, see in Figure 19, the peaks of amine (CH_2-NH_2) and nitrile (C≡N) have the same position at 399.3 eV (Sylvestre et al. 2004; Moulijn and Building 1995; Hellgren et al. 2005), and the peak at 402.9 eV is belonging to ammonium ion (-NH_3^+) or hydroxylamine (Hellgren et al. 2005; Chang et al. 2013). The NH_3^+ peak could be observed, due to the protonation with the acid during the hydrolysis. Even though chloric acid was employed in the reaction, however, the chloride ion attached on the ammonium was exchanged by hydroxide ion (OH^-) during the filtration and rinse process; that explains the absence of chlorine on XPS survey.

In general, the anime conversion was successfully proceeded, with the evidence from the presence of Al in XPS survey and the hydroxylamine in high-resolution XPS. Although the hydrolysis was not completely exploited in the process, the amine product could be achieved lager by adding extra chloric acid solution in the step, as a suggestion. Nevertheless, the number of amine group, achieved in the conversion reaction, could be identified and quantified by either titration method or IR analysis, as a suggestion. In addition, the dissimilarities between FG-CN and FG-NH_2 samples are compared via the signals from high-resolution XPS in both C1s and N1s, see in figure Graph 8 and Graph 9 in appendix III, respectively; these figures present visibly the impact from amine conversion, which is observed as a lump in C1s and a ramp in N1s.

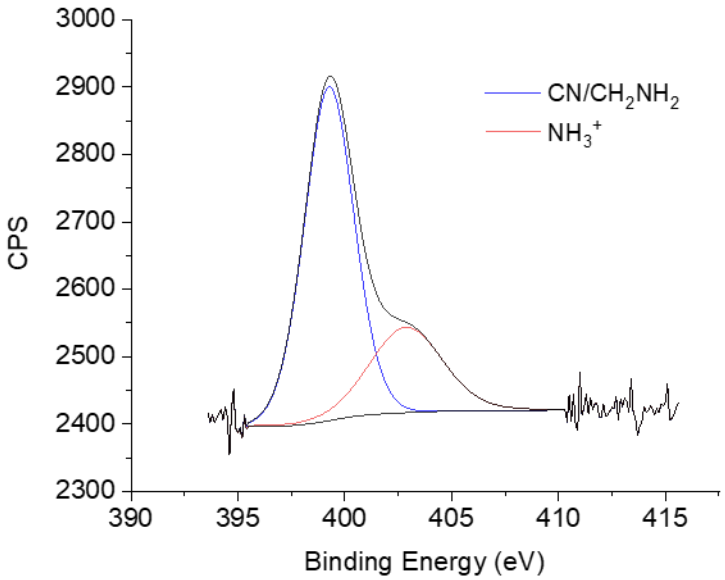

FIGURE 19: Sample from amine conversion in high-resolution XPS in N1s

5 COMPOSITE MATERIAL OF GRAPHENE AND POLYURETHANE

The interest and purpose of the project is to combine the functional graphene with polyurethane (PUR) for a new advanced material in strength and conductivity in the future work. There are three components in PUR, containing polyol, isocyanate and a catalyst. In the incorporation materials process, the functional graphene powder was firstly dispersed in polyol before adding in isocyanate and a catalyst. The composite material, then, was molded as small bones, see in Figure 20, and they were characterized in the mechanical test by checking the E modulus (Young's modulus) and the ultimate tensile strength (UTS). The E modulus is quantity determining object resistance as the slope of its stress–strain curve; in which the stepper of the slope is, the bigger value of E modulus gain, meaning the stiffness improvement of the material. While the UTS is defined by the maximum stress of the material under a load before the object is broken.

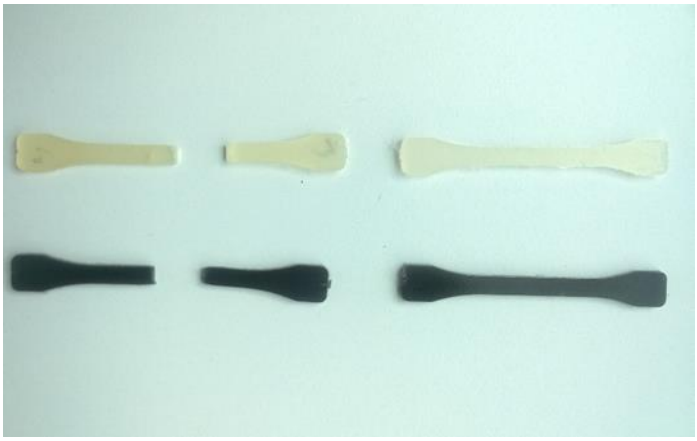

FIGURE 20: The bones samples of pure PUR (upper) and composite material with 0.1% graphene (lower)

The tensile strength test of all samples, including exfoliated graphene (EG), benzyl ethanol functional graphene (EG-EOH) and graphene with brushes (EG-P), are compared with the control sample made from pure polyurethane (PUR), see in Figure 21, in which only 0.1% of graphene in mass was used for molding. Due to the limit time of the project and the similar property in strength of methanol and ethanol, the sample with phenethyl alcohol as the functional group on graphene was used, because of its earlier success in growing brushes on graphene. The benzyl alcohol composite is expected to have a little higher quality than the phenethyl alcohol composite. Furthermore, the graphene with polymer brushes (EG-P)

would have same features, regardless of the group from benzyl diazonium salt. Because of the overwhelmingly amount of the monomer grown from the functional groups, the polymer brush would give the effect to the composite material, instead of impact by the functional group.

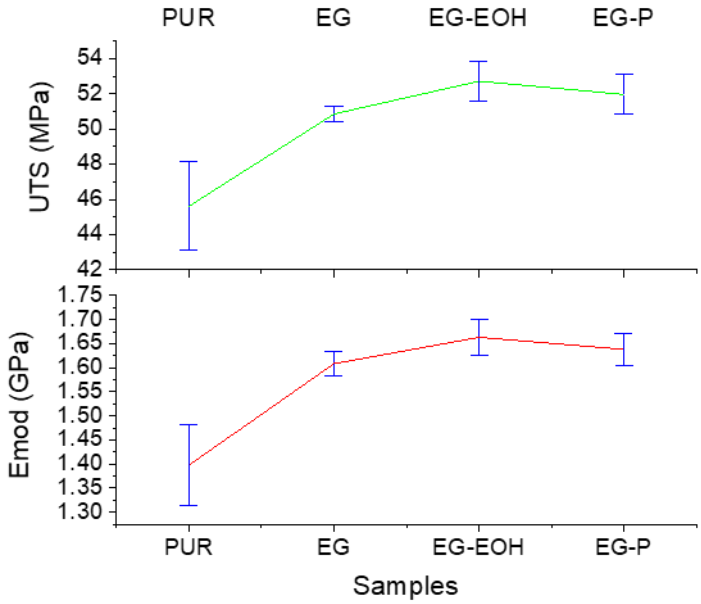

FIGURE 21: Tensile strength comparison of all samples, pure PUR (PUR), exfoliated graphene (EG), benzyl ethanol functional graphene (EG-EOH) and graphene with brushes (EG-P). The green line is ultimate tensile strength and the red line is E modulus (Young's modulus)

The graphene content supports for the material strength. Based on the survey, the strength of sample EG-EOH is the highest one. While the EG-P sample has a similar strength with EG, meaning that the polymer bush might either lower the strength of the composite or have less graphene sheet than EG-EOH, due to its high molecular mass, provided from the brushes. By the direct connection, the properties of graphene sheet could influence the composite straightly via functional groups and polymer brushes. In EG sample, because there is no "bridge" connecting between graphene and the mixture polymer, hence the graphene could support the material lightly. While in EG-P, beside the similar effect of graphene to isocyanate like in EG sample, the polymer could link the graphene with isocyanate and lead the impact of graphene directly through brushes. That is also applied to EG-OH the connection could be transferred through the functional groups, however the results of EG-OH and EG-P were different.

One of the possibilities that EG-P has lower strength than EG-OH is the length of the direct connection between graphene and the isocyanate. In EG-P sample, the long brushes on the graphene tend to lessen the impact from the graphene sheet to the polymeric network, due to the long chain carbon, causing loss of the connection. In contrary, the EG-EOH with a short connection between graphene and isocyanate,

this could develop the association of graphene and the commercial polymer. In a consideration, if brushes are grown with an optimal length on graphene, the connection from the graphene to the polymeric network could be improved and that might be better than the impact of functional graphene to the composites. Because a brush could offer multiple bonds with isocyanate, and that is the way graphene can influence to the polymeric network directly, leading to a high quality of the product. However, the differences between samples with graphene content, comprising EG, EG-EOH and EG-P, are similar to each other, hence the functional group and polymer brushes from those samples could not strengthen much for the composite material.

Nevertheless, due to the small number of functional groups on graphene, the difference is not large in comparison between EG-EOH and EG. From that the higher functionalization on graphene is expected to give a higher strength for the composite material. Furthermore, the concentration of graphene in composite material also effects to the strength of composite material. In EG samples, the higher concentration of graphene put in, the harder the material is in both E modulus and Ultimate tensile. While in EG-OH the E modulus is increased, however the Ultimate tensile is decreased, see in Graph 7 in appendix III.

6 CONCLUSION AND PROSPECTS

As the main idea of making a new composite material based on graphene and polyurethane (PUR). There are two methods of functional graphene production, namely graphene exfoliation (EG) and fluorographene (FG), which have been focused and learned in this project. The functional graphene from EG was processed forward to mix with PUR.

In the study of EG, functionalization was carried out successfully in one-pot process where the benzyl alcohol diazonium salt was dissolved in electrolyte. Due to the oxidative electrochemical exfoliation, the graphene was influenced and that caused many defects on graphene by impurities instead of the functional groups. The defects measured by Raman presented roughly 442 carbon atoms per defect, including functional groups impurities and other defect factors on the graphene. Chlorination reaction was employed to convert the OH^- group of functional groups to Cl^-, the result is steady for 24 hour of reaction time. Moreover, by counting the chlorine content after the chlorination experiment, the number of potential brushes could be calculated by the XPS analysis which indicated one latent functional group per around 900 carbons. The XPS technique was applied again to define the content of polymerized sample (EG-P), in which the chlorine content was lost, due to its very tiny amount. The thermal gravity analysis is recommended to determine the presence of polymer brushes on functional graphene in future.

In FG experimental, the cyanidation FG process consists of two processes, pretreatment with sonication and functionalization by cyanide salt reaction. In the sonication stage, the graphite fluoride could be treated to prepare FG. It is noticeable that the more FG could be produced, the better the reaction with cyanide salt become. By choosing the type of the sonicator, controlling a low FG concentration in DMF and operating a high output power for sonication, these adjustments could give more FG product, which could support in the cyanine reaction in producing FG-CN. In the functionalization, two types of cyanide salts, KCN and TBA, were used in this reaction. Basing on the data from XPS analysis, the TBA salt, achieving 36.7 carbon atoms per functional group, showing the higher efficiency than KCN, attaining 40 to 50 carbon atoms per functional group. In defluorination, TBA salt could reduce a larger amount of fluorine atom out of FG, suggesting that due to the willing-leaving CN^- group in TBA, the reaction is developed. Therefore, the survival of CN^- in solution is supposed to be the key the efficiency of the reaction, which could prolong or give more chance for the S_N2 reaction occurrence on FG. Furthermore, the changing procedure in washing step, by using filtration, was more efficient and more yield than the original procedure, using centrifugation with various solvents.

The amine conversion for FG-CN was successfully implemented; however, the hydrolysis step should be improved to obtain more FG-NH_2 product. During the hydrolysis stage, an addition water or acid solution might be charged in the reaction, so that the compounds could avoid the aggregation and precipitation, prolonging the survival of chemicals for the reaction. The IR-FTR with Germanium crystal should be employed to distinguish cyano group and amine group, besides, titration method is suggested to estimate the number of amine groups on the sample, also confirm the success of the conversion reaction.

In comparison between two functionalization methods, the number of functional groups from FG is much higher than the EG, however, both the condition and time for reactions in EG is faster and simpler. Both methods could be developed to obtain more product in functionalization by modifying some factors in the reactions. Particularly, the reductive exfoliation (Ejigu, Kinloch, and Dryfe 2017) could be employed in EG to avoid the defects from oxidation and the applied voltage could also be adjusted to gain the optimal functional group on graphene. While in FG, the reaction with cyanide salts, the survival of reactants should be considered, due to the sediment in the end of reaction. Hence, new solvents which could dissolve both FG and salt are commended, or an ideal mixed solvent also is an option.

In composite materials, the appearance of graphene content in composite samples influences explicitly to the hardness of the material, compared with the pure PUR sample. In detail, the composite from functional graphene (EG-EOH) shows the highest tensile strength, while the one mixed with polymerized graphene (EG-P) is a bit lower in tensile strength. This proves that the brushes might not help to improve the higher strength for composites, however, the length of the brushes should be considered for the stronger composites. Because the connection of graphene sheets with polymeric network is suggested to be decreased, due to the long brushes. Besides, due of the better quality of the composite from EG-EOH and EG-P, compared with the composite from EG, the functional groups on graphene could reinforce the stiffness of the composite material, leading to the more functional groups on graphene, the better quality of composite. Nevertheless, depending on the desired products, the yield of functionalization might obstruct graphene properties to the composites, resulting to the low quality of the product.

Moreover, the addition concentration of graphene content in composite material could increase the tensile strength of the material; however, the change is slightly. In industrial, the concentration of graphene content should be taken into account of the cost effect, in which the product quality is not worth as its cost. Therefore, all features of the composite material, containing the number of functional groups on graphene, the length of brushes and the concentration of graphene content in composites, should be

adjusted and modified to gain the optimal value for the desire products in the end. In the future, the functional graphene could be undergone conductivity tests for employing in conductive material for electronic devices.

REFERENCES

Achee, Thomas C., Wanmei Sun, Joshua T. Hope, Samuel G. Quitzau, Charles Brandon Sweeney, Smit A. Shah, Touseef Habib, and Micah J. Green. 2018. 'High-Yield Scalable Graphene Nanosheet Production from Compressed Graphite Using Electrochemical Exfoliation'. Scientific Reports 8 (1): 1–8.

Allongue, Philippe, Michel Delamar, Bernard Desbat, Olivier Fagebaume, Rachid Hitmi, Jean Pinson, and Jean Michel Savéant. 1997. 'Covalent Modification of Carbon Surfaces by Aryl Radicals Generated from the Electrochemical Reduction of Diazonium Salts'. Journal of the American Chemical Society 119 (1): 201–7.

Amiri, Ahmad, Mohammad Naraghi, Goodarz Ahmadi, Mohammadreza Soleymaniha, and Mehdi Shanbedi. 2018. 'A Review on Liquid-Phase Exfoliation for Scalable Production of Pure Graphene, Wrinkled, Crumpled and Functionalized Graphene and Challenges'. FlatChem 8 (January): 40–71.

Bakandritsos, Aristides, Martin Pykal, Piotr Boński, Petr Jakubec, Demetrios D. Chronopoulos, Kateřina Poláková, Vasilios Georgakilas, et al. 2017. 'Cyanographene and Graphene Acid: Emerging Derivatives Enabling High-Yield and Selective Functionalization of Graphene'. ACS Nano 11 (3): 2982–91.

Barès, Hugo, Aristides Bakandritsos, Miroslav Medveď, Juri Ugolotti, Petr Jakubec, Ondřej Tomanec, Sergii Kalytchuk, Radek Zbořil, and Michal Otyepka. 2019. 'Bimodal Role of Fluorine Atoms in Fluorographene Chemistry Opens a Simple Way toward Double Functionalization of Graphene'. Carbon 145: 251–58.

Besenhard, J. O. 1976. 'The Electrochemical Preparation and Properties of Ionic Alkali Metal-and NR4-Graphite Intercalation Compounds in Organic Electrolytes'. Carbon 14 (2): 111–15.

Biesheuvel, P. M., and J. E. Dykstra. 2018. 'The Difference between Faradaic and Nonfaradaic Processes in Electrochemistry', 1–10.

Bond, A. M., M. Fleischmann, and J. Robinson. 1984. 'Electrochemistry in Organic Solvents without Supporting Electrolyte Using Platinum Microelectrodes'. Journal of Electroanalytical Chemistry 168 (1–2): 299–312.

Brownson, Dale A.C., and Craig E. Banks. 2014. 'Introduction to Graphene'. The Handbook of Graphene Electrochemistry, 1–201.

Bumbrah, Gurvinder Singh, and Rakesh Mohan Sharma. 2016. 'Raman Spectroscopy – Basic Principle, Instrumentation and Selected Applications for the Characterization of Drugs of Abuse'. Egyptian Journal of Forensic Sciences 6 (3): 209–15.

Chang, Yunzhen, Gaoyi Han, Jinping Yuan, Dongying Fu, Feifei Liu, and Sidian Li. 2013. 'Using Hydroxylamine as a Reducer to Prepare N-Doped Graphene Hydrogels Used in High-Performance Energy Storage'. Journal of Power Sources 238: 492–500.

Chen, Xiaoyi, Li Yuan, Pengyuan Yang, Jianhua Hu, and Dong Yang. 2011. 'Covalent Polymeric Modification of Graphene Nanosheets via Surface-Initiated Single-Electron-Transfer Living Radical Polymerization'. Journal of Polymer Science, Part A: Polymer Chemistry 49 (23): 4977–86.

Chronopoulos, Demetrios D., Aristides Bakandritsos, Martin Pykal, Radek Zbořil, and Michal Otyepka. 2017. 'Chemistry, Properties, and Applications of Fluorographene'. Applied Materials Today 9: 60–70.

Daasbjerg, Kim, Stefan Urth Nielsen, Steen U. Pedersen, Line Koefoed, and Henning Lund. 2016. 'Wohl-Ziegler Bromination of Electrografted Films for Optimizing Atom Transfer Radical Polymerization'. Electroanalysis 28 (11): 2849–54.

Dorn, M., P. Lange, A. Chekushin, N. Severin, and J. P. Rabe. 2010. 'High Contrast Optical Detection of Single Graphenes on Optically Transparent Substrates'. Journal of Applied Physics 108 (10): 87–90.

Dresselhaus, Mildred S., Ado Jorio, Mario Hofmann, Gene Dresselhaus, and Riichiro Saito. 2010. 'Perspectives on Carbon Nanotubes and Graphene Raman Spectroscopy'. Nano Letters 10 (3): 751–58.

Dubecký, Matúš, Eva Otyepková, Petr Lazar, František Karlický, Martin Petr, Klára Čépe, Pavel Banáš, Radek Zbořil, and Michal Otyepka. 2015. 'Reactivity of Fluorographene: A Facile Way toward Graphene Derivatives'. Journal of Physical Chemistry Letters 6 (8): 1430–34.

Ejigu, Andinet, Ian A. Kinloch, and Robert A.W. Dryfe. 2017. 'Single Stage Simultaneous Electrochemical Exfoliation and Functionalization of Graphene'. ACS Applied Materials and Interfaces 9 (1): 710–21.

Englert, Jan M., Philipp Vecera, Kathrin C. Knirsch, Ricarda A. Schäfer, Frank Hauke, and Andreas Hirsch. 2013. 'Scanning-Raman-Microscopy for the Statistical Analysis of Covalently Functionalized Graphene'. ACS Nano 7 (6): 5472–82.

Enoki, Toshiaki, Nikhil Koratkar, Juan M.D. Tascon, Robert H. Hurt, Chong Rae Park, Alberto Bianco, Marc Monthioux, et al. 2013. 'All in the Graphene Family – A Recommended Nomenclature for Two-Dimensional Carbon Materials'. Carbon 65: 1–6.

Feng, Wei, Peng Long, Yi Yu Feng, and Yu Li. 2016. 'Two-Dimensional Fluorinated Graphene: Synthesis, Structures, Properties and Applications'. Advanced Science 3 (7): 1–22.

Ferrari, Andrea C, and Denis M Basko. 2013. 'Raman Spectroscopy as a Versatile Tool for Studying

the Properties of Graphene.' Nature Nanotechnology 8 (4): 235–46.

Greczynski, G., and L. Hultman. 2019. 'X-Ray Photoelectron Spectroscopy: Towards Reliable Binding Energy Referencing'. Progress in Materials Science, 100591.

Gu, Si Yong, Chien Te Hsieh, Jun Yao Yuan, Jen Hao Hsueh, and Yasser Ashraf Gandomi. 2018. 'Amino-Functionalization of Graphene Nanosheets by Electrochemical Exfoliation Technique'. Diamond and Related Materials 87 (May): 99–106.

Gupta, Satyendra C., and James T. Taguchi. 1982. 'Pacemaker Catheter- Induced Systolic Murmur'. Angiology 33 (4): 277–79.

Haldar, Soumyajyoti, and Biplab Sanyal. 2016. 'Defects in Graphene and Its Derivatives'. Intech, 8–12.

Hartmann, Markus A., Melanie Todt, Franz G. Rammerstorfer, Franz D. Fischer, and Oskar Paris. 2013. 'Elastic Properties of Graphene Obtained by Computational Mechanical Tests'. Epl 103 (6).

He, Kai, Guiqiu Chen, Guangming Zeng, Min Peng, Zhenzhen Huang, Jiangbo Shi, and Tiantian Huang. 2017. 'Stability, Transport and Ecosystem Effects of Graphene in Water and Soil Environments'. Nanoscale 9 (17): 5370–88.

Hellgren, Niklas, Jinghua Guo, Yi Luo, Conny Såthe, Akane Agui, Stepan Kashtanov, Joseph Nordgren, Hans Ågren, and Jan Eric Sundgren. 2005. 'Electronic Structure of Carbon Nitride Thin Films Studied by X-Ray Spectroscopy Techniques'. Thin Solid Films 471 (1–2): 19–34.

Hernandez, Yenny, Valeria Nicolosi, Mustafa Lotya, Fiona M. Blighe, Zhenyu Sun, Sukanta De, I. T. McGovern, et al. 2008. 'High-Yield Production of Graphene by Liquid-Phase Exfoliation of Graphite'. Nature Nanotechnology 3 (9): 563–68.

Hibbert, D. Brynn. 1993. 'Introduction to Electrochemistry'. Macmillan Physical Science Series, no. Introduction to electrochemistry.: 1–10.

I. Mikheeva, S. M. Arkhipov, and A. E. Pruntsev V. 1972. 'Solubility Of Aluminum Lithium Hydride In The Systems Lia1h 4 -Ether-Benzene And Lia1h 4 -Ether-Toluene At 25°'. A Division of Plenum Publishing Corporation 139 (12): 66–89.

Jacobberger, Robert M., Rushad Machhi, Jennifer Wroblewski, Ben Taylor, Anne Lynn Gillian-Daniel, and Michael S. Arnold. 2015. 'Simple Graphene Synthesis via Chemical Vapor Deposition'. Journal of Chemical Education 92 (11): 1903–7.

JOHN W. BAKER and D. N. BAILE. 1957. 'The Mechanism of the Reaction of AryE IsoCyanates with Alcohols and Amines. The Spontaneous '' Reaction with Amines.' Journal of the Chemical Society, no. 4652: 4652–62.

Jorio, A, E H Martins Ferreira, F Stavale, C A Achete, R B Capaz, M V O Moutinho, A Lombardo, T

S Kulmala, and A C Ferrari. 2011. 'Cancado_Ferrari_Nanoletters_2011_Quantifying Defect in Graphene via Raman at Different Excitation Energies.Pdf'. Nano Letters, 3190–96.

Jorio, Ado, Erlon H. Martins Ferreira, Luiz G. Cançado, Carlos A. Achete, and Rodrigo B. Capaz. 2009. 'Measuring Disorder in Graphene with Raman Spectroscopy'. Physics and Applications of Graphene - Experiments, 439–54.

Jussila, Henri, Tom Albrow-Owen, He Yang, Guohua Hu, Sinan Aksimsek, Niko Granqvist, Harri Lipsanen, Richard C.T. Howe, Zhipei Sun, and Tawfique Hasan. 2017. 'New Approach for Thickness Determination of Solution-Deposited Graphene Thin Films'. ACS Omega 2 (6): 2630–38.

K. S. Novoselov, 1 A. K. Geim, 1* S. V. Morozov, 2 D. Jiang, 1 Y. Zhang, 1 S. V. Dubonos, 2 I. V. Grigorieva, 1 A. A. Firsov2. 2004. 'Electric Field Effect in Atomically Thin Carbon Films' 306 (1): 666–69.

Kaciulis, Saulius, A. Mezzi, P. Calvani, and D. M. Trucchi. 2014. 'Electron Spectroscopy of the Main Allotropes of Carbon'. Surface and Interface Analysis 46 (10–11): 966–69.

Karlický, František, Radek Zbořil, and Michal Otyepka. 2012. 'Band Gaps and Structural Properties of Graphene Halides and Their Derivates: A Hybrid Functional Study with Localized Orbital Basis Sets'. Journal of Chemical Physics 137 (3).

Kuila, Tapas, Saswata Bose, Ananta Kumar Mishra, Partha Khanra, Nam Hoon Kim, and Joong Hee Lee. 2012. 'Chemical Functionalization of Graphene and Its Applications'. Progress in Materials Science 57 (7): 1061–1105.

Lai, Wenchuan, Yuehui Yuan, Xu Wang, Yang Liu, Yulong Li, and Xiangyang Liu. 2017. 'Radical Mechanism of a Nucleophilic Reaction Depending on a Two-Dimensional Structure'. Physical Chemistry Chemical Physics 20 (1): 489–97.

Lee, Changgu, Xiaoding Wei, Jeffrey W. Kysar, and James Hone. 2008a. 'Measurement of the Elastic Properties and Intrinsic Strength of Monolayer Graphene'. Science 321 (5887): 385–88.

Lee, Changgu, Xiaoding Wei, Jeffrey W Kysar, and James Hone. 2008b. 'Of Monolayer Graphene'. Science (New York, N.Y.) 321 (July): 385–88.

Lemal, David M. 2004. 'Perspective on Fluorocarbon Chemistry'. Journal of Organic Chemistry 69 (1): 1–11.

Levere, Martin E., Nga H. Nguyen, Xuefei Leng, and Virgil Percec. 2013. 'Visualization of the Crucial Step in SET-LRP'. Polymer Chemistry 4 (5): 1635–47.

Lin Li-Shang, Aidan Westwood, Rik Brydson. 2016. 'Graphene Synthesis Via Electrochemical Exfoliation of Graphite Nanoplatelets in Aqueous Sulphuric Acid'. University of Leeds, 1–6.

Lligadas, Gerard, Silvia Grama, and Virgil Percec. 2017. 'Recent Developments in the Synthesis of

Biomacromolecules and Their Conjugates by Single Electron Transfer-Living Radical Polymerization'. Biomacromolecules 18 (4): 1039–63.

Malard, L. M., M. A. Pimenta, G. Dresselhaus, and M. S. Dresselhaus. 2009. 'Raman Spectroscopy in Graphene'. Physics Reports 473 (5–6): 51–87.

Matochová, Dagmar, Miroslav Medved, Aristides Bakandritsos, Tomáš Steklý, Radek Zbořil, and Michal Otyepka. 2018. '2D Chemistry: Chemical Control of Graphene Derivatization'. Journal of Physical Chemistry Letters 9 (13): 3580–85.

Mattalia, J.-M., A. Samat, and M. Chanon. 1991. ' First Observation of a C–CN Bond Cleavage during the Reduction of a Nitrile with LiAlH 4 : A S.E.T. Reaction? '. J. Chem. Soc., Perkin Trans. 1, no. 7: 1769–70.

Matyjaszewski, Krzysztof. 2012. 'Atom Transfer Radical Polymerization (ATRP): Current Status and Future Perspectives'. Macromolecules 45 (10): 4015–39.

Medveď, Miroslav, Giorgio Zoppellaro, Juri Ugolotti, Dagmar Matochová, Petr Lazar, Tomáš Pospíšil, Aristides Bakandritsos, Jiří Tuček, Radek Zbořil, and Michal Otyepka. 2018. 'Reactivity of Fluorographene Is Triggered by Point Defects: Beyond the Perfect 2D World'. Nanoscale 10 (10): 4696–4707.

Moulijn, J A, and Bedson Building. 1995. 'Evolution of Nitrogen Functionalities In'. Carbon 33 (11): 1641–53.

Noh, Ye Ji, Han Ik Joh, Jaesang Yu, Soon Hyoun Hwang, Sungho Lee, Cheol Ho Lee, Seong Yun Kim, and Jae Ryoun Youn. 2015. 'Ultra-High Dispersion of Graphene in Polymer Composite via Solvent Free Fabrication and Functionalization'. Scientific Reports 5: 1–7.

Oldham, Keith B. 2010. 'Fractional Differential Equations in Electrochemistry'. Advances in Engineering Software 41 (1): 9–12.

Ossonon, Benjamin Diby, and Daniel Bélanger. 2016. 'Functionalization of Graphene Sheets by the Diazonium Chemistry during Electrochemical Exfoliation of Graphite'. Carbon 111: 83–93.

Ossonon, Benjamin Diby Bélanger, Daniel. 2017. 'Synthesis and Characterization of Sulfophenyl-Functionalized Reduced Graphene Oxide Sheets'. RSC Advances 7 (44): 27224–34.

Parvez, Khaled, Zhong Shuai Wu, Rongjin Li, Xianjie Liu, Robert Graf, Xinliang Feng, and Klaus Müllen. 2014. 'Exfoliation of Graphite into Graphene in Aqueous Solutions of Inorganic Salts'. Journal of the American Chemical Society 136 (16): 6083–91.

Parvez, Khaled, Sheng Yang, Xinliang Feng, and Klaus Müllen. 2015. 'Exfoliation of Graphene via Wet Chemical Routes'. Synthetic Metals 210: 123–32.

Paton, Keith R., Eswaraiah Varrla, Claudia Backes, Ronan J. Smith, Umar Khan, Arlene O'Neill, Conor Boland, et al. 2014. 'Scalable Production of Large Quantities of Defect-Free Few-Layer

Graphene by Shear Exfoliation in Liquids'. Nature Materials 13 (6): 624–30.

Pruntsev, A. E., S. M. Arkhipov, and V. I. Mikheeva. 1972. 'Solubility in the Systems AlCl3-LiCl-Ether, AlCl3-LiCl-Toluene, and AlBr3-NaBr-Toluene at 25°c'. Bulletin of the Academy of Sciences of the USSR Division of Chemical Science 21 (12): 2581–85.

Robinson, Jeremy T., James S. Burgess, Chad E. Junkermeier, Stefan C. Badescu, Thomas L. Reinecke, F. Keith Perkins, Maxim K. Zalalutdniov, et al. 2010. 'Properties of Fluorinated Graphene Films'. Nano Letters 10 (8): 3001–5.

Rodriguez, Deana A., and Ronny Priefer. 2014. 'Sulfite Formation versus Chlorination of Benzyl Alcohols with Thionyl Chloride'. Tetrahedron Letters 55 (19): 3045–48.

Sofo, Jorge O., Ajay S. Chaudhari, and Greg D. Barber. 2007. 'Graphane: A Two-Dimensional Hydrocarbon'. Physical Review B - Condensed Matter and Materials Physics 75 (15): 1–4.

Stapleton, Andrew J, Cameron J Shearer, Christopher T Gibson, Ashley D Slattery, and Joseph G Shapter. 2016. 'Accurate Thickness Measurement of Graphene'. Nanotechnology 27 (12): 125704.

Steven Farmer. 2019. 'Conversion of Nitriles to 1° Amines Using LiAlH4'. In , 5366. chem libretexts.

Stormer, H.L., P. Kim, K.J. Sikes, G. Fudenberg, J. Hone, K.I. Bolotin, Z. Jiang, and M. Klima. 2008. 'Ultrahigh Electron Mobility in Suspended Graphene'. Solid State Communications 146 (9–10): 351–55.

Suchtelen, J. van. 1972. 'Product Properties: A New Application of Composite Materials'. Philips Research Report 27: 28–37.

Sun, Lili, Guisheng Peng, Hongmei Niu, Qiang Wang, and Chunbao Li. 2008. 'A Highly Chemoselective and Rapid Chlorination of Benzyl Alcohols under Neutral Conditions'. Synthesis, no. 24: 3919–24.

Sylvestre, Jean Philippe, Suzie Poulin, Andrei V. Kabashin, Edward Sacher, Michel Meunier, and John H.T. Luong. 2004. 'Surface Chemistry of Gold Nanoparticles Produced by Laser Ablation in Aqueous Media'. Journal of Physical Chemistry B 108 (43): 16864–69.

T.H.Flemban. 2017. 'High Quality Zinc Oxide Thin Films and Nanostructures Prepared by Pulsed Laser Deposition for Photodetectors'.

Teweldebrhan, Desalegne, Chun Ning Lau, Suchismita Ghosh, Alexander A. Balandin, Wenzhong Bao, Irene Calizo, and Feng Miao. 2008. 'Superior Thermal Conductivity of Single-Layer Graphene'. Nano Letters 8 (3): 902–7.

Withers, F., M. Dubois, and A. K. Savchenko. 2010. 'Electron Properties of Fluorinated Single-Layer Graphene Transistors'. Physical Review B - Condensed Matter and Materials Physics 82 (7): 1–4.

Wu, Hang, Weifeng Zhao, Huawen Hu, and Guohua Chen. 2011. 'One-Step in Situ Ball Milling

Synthesis of Polymer-Functionalized Graphene Nanocomposites'. Journal of Materials Chemistry 21 (24): 8626–32.

Wu, Jingjie, Pranav P. Sharma, Bradley H. Harris, and Xiao Dong Zhou. 2014. 'Dioxide: IV Dependence of the Faradaic Efficiency and Current Density on the Microstructure and Thickness of Tin Electrode'. Journal of Power Sources 258: 189–94.

Yang, Yang, Guolin Lu, Yongjun Li, Zhanzhan Liu, and Xiaoyu Huang. 2013. 'One-Step Preparation of Fluorographene: A Highly Efficient, Low-Cost, and Large-Scale Approach of Exfoliating Fluorographite'. ACS Applied Materials and Interfaces 5 (24): 13478–83.

Yang, Yingchang, Hongshuai Hou, Guoqiang Zou, Wei Shi, Honglei Shuai, Jiayang Li, and Xiaobo Ji. 2019. 'Electrochemical Exfoliation of Graphene-like Two-Dimensional Nanomaterials'. Nanoscale 11 (1): 16–33.

Zheng, Wenge, Bin Shen, and Wentao Zhai. 2013. 'Surface Functionalization of Graphene with Polymers for Enhanced Properties'. New Progress on Graphene Research.

Zhu, Mingshan, Xiaodong Xie, Yunlong Guo, Penglei Chen, Xiaowei Ou, Gui Yu, and Minghua Liu. 2013. 'Fluorographene Nanosheets with Broad Solvent Dispersibility and Their Applications as a Modified Layer in Organic Field-Effect Transistors'. Physical Chemistry Chemical Physics 15 (48): 20992–0.

APPENDICES

Appendix I: Procedure and table

Raman Sample Preparation

A small amount of graphene powder around 1 mg is dispersed in 10 ml DMF to have a fine suspension of graphene. A petri dish glass is used to contain MilliQ water, filled more than a half height of the glass. 1 ml of graphene solution is injected to the MilliQ water from the bottom of the glass by a syringe and a needle. Then, a few dropwise of ethyl acetate is carefully pipetted from the walls of the glass, so that the ethyl acetate can slide and spread over on the top of the surface of water. The acetone helps to cool down the top surface and transferred downward, due to the convection, while the graphene in solution is shifted to the top surface of water and form a thin firm on the surface. A small fragment of SiO2 is used to pick up the graphene, being ready for analysis.

Comparison the amount of oxygen and chlorine among samples from processes EG, chlorination and polymerization in XPS survey spectrum

Samples	Oxygen (%)	Chlorine (%)
EG-OH	12.04	0
EG-Cl	9.98	0.1
EG-P	11.4	0

Appendix II: Equations and calculations

Raman Calculation

$$\frac{I_D}{I_G} = C_A \frac{r_A^2 - r_S^2}{r_A^2 - 2r_S^2}\left[\exp\left(-\frac{\pi r_S^2}{L_D^2}\right) - \exp\left(-\frac{\pi(r_A^2 - r_S^2)}{L_D^2}\right)\right] + C_S\left[1 - \exp\left(-\frac{\pi r_S^2}{L_D^2}\right)\right]$$

Exchanging all available value to the equation to calculate the L_D

$$1.1 = 4.56\ x\ \frac{1^2 - 0.07^2}{1^2 - 2\ x\ 0.07^2}\left[\exp\left(-\frac{\pi 0.07^2}{L_D^2}\right) - \exp\left(-\frac{\pi(1^2 - 0.07^2)}{L_D^2}\right)\right] + 0.86\ x\ \left[1 - \exp\left(-\frac{\pi 0.07^2}{L_D^2}\right)\right]$$

The L_D result:

$$L_D = 3.36\ (nm) = 3.36 \times 10^{-7}\ (cm)$$

Finding σ

$$L_D = \frac{1}{\sqrt{\sigma}} <=> \sigma = 8.86\ x\ 10^{12}\ (cm^{-2})$$

σ converted to mol/cm^{-2} by dividing by Avogadro's number, N_A (6.02 x 10^{23} mol/cm^{-2}):

$$\sigma = 1.47\ x\ 10^{11}\ (mol/cm^{-2})$$

Inferring the number of carbons per a defect is calculated by dividing the atom surface density of carbon:

$$\frac{6.5\ x\ 10^{-9}}{\sigma} = 442\ carbons\ atoms\ per\ defect$$

Equation for calculating the number of functional groups on fluorographene

$$\frac{C}{N} = \frac{C1s\ \% - N1s\ \%}{N1s\ \%}$$

Where C is number of carbon atoms and N is number of nitrogen atoms on sample. Because, the cyano group have one carbon atom is the group, hence the number of carbon atom on graphene is equal to the subtraction of total carbon and carbon from nitrile.

Appendix III: Graphs and figures

Graph 1: Polymer bush on graphene in high-resolution XPS

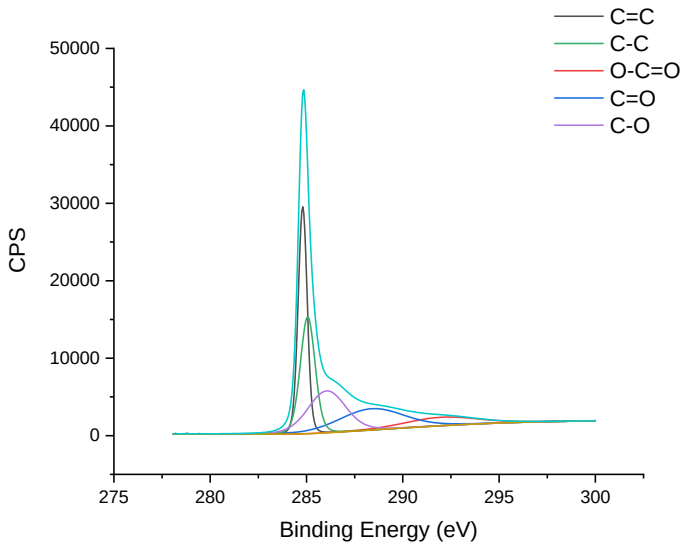

Graph 2: Graphite fluoride control sample in high-resolution XPS

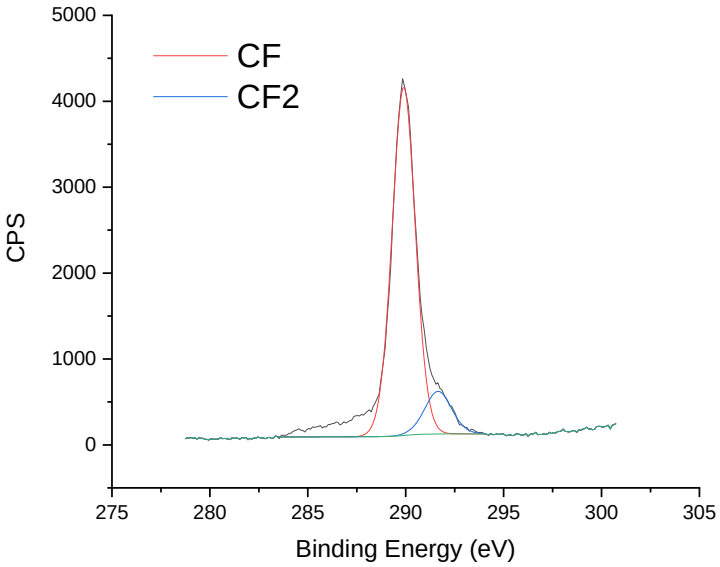

Graph 3: Graph of cyanographene from short-term process in high-resolution XPS

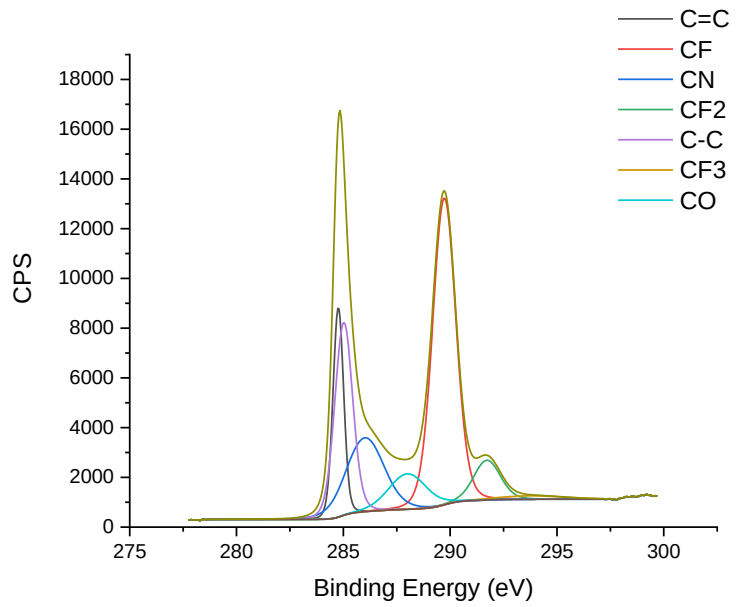

Graph 4: Graph of cyanographene from long-term process in high-resolution XPS

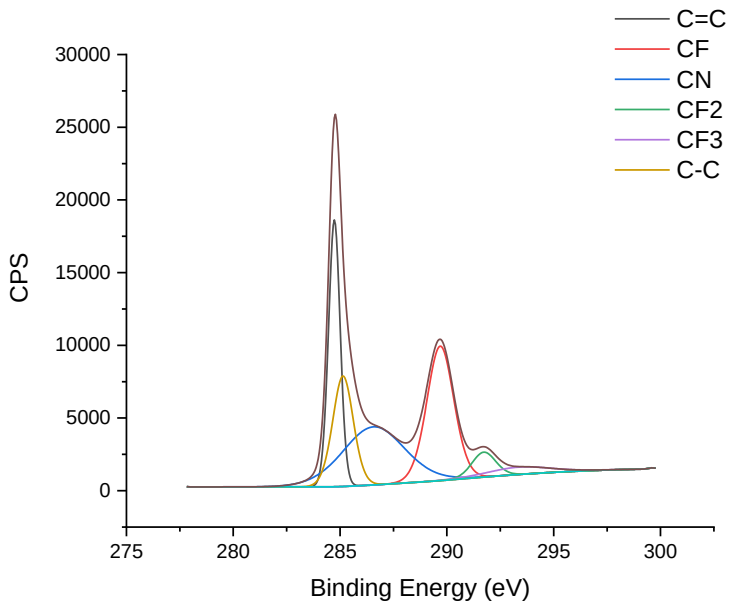

Graph 5: Graph of cyanographene from wet solvent in high-resolution XPS

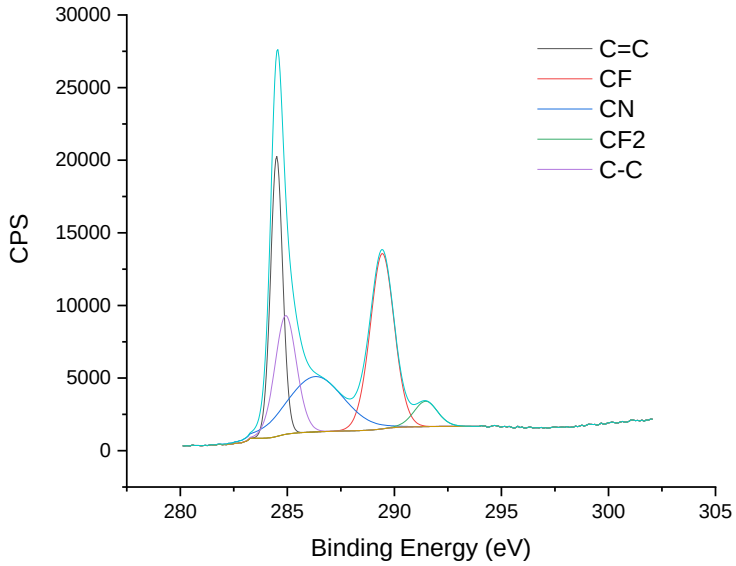

Graph 6: Graph of cyanographene from reaction with Tetrabutylammonium cyanine in high-resolution XPS

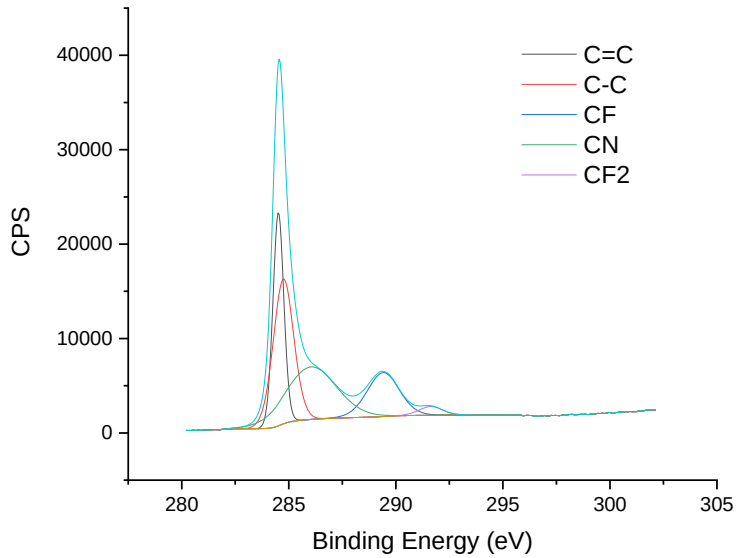

Graph 7: The comparison of the tensile strength of EG and EG-EOH in different concentration of graphene in the composite material. The red lines are from EG and the blue lines are from EG-EOH

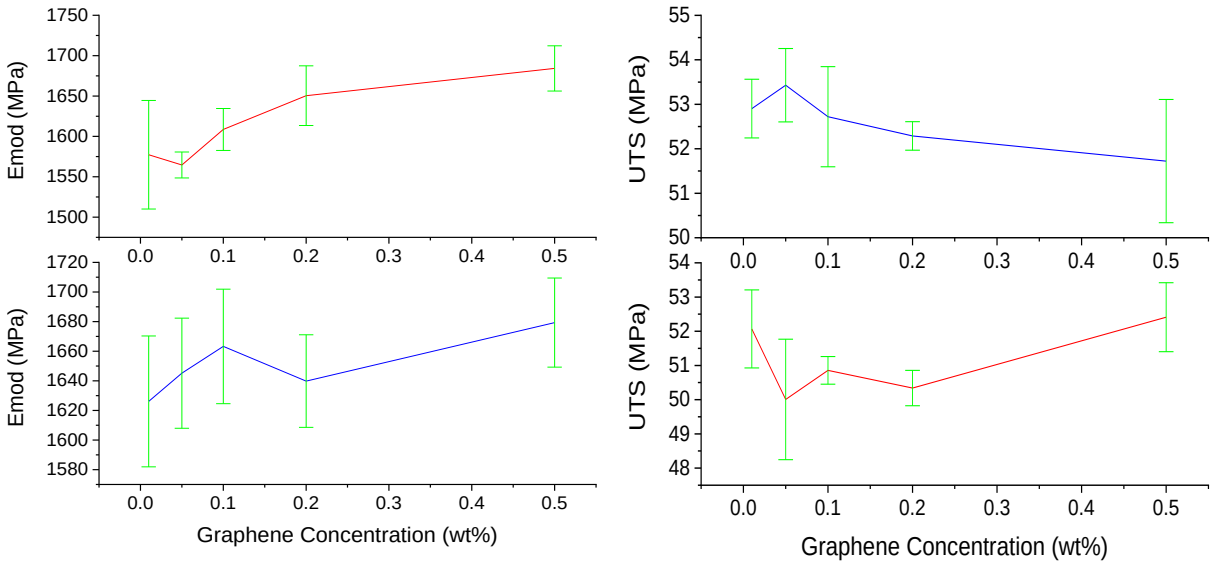

Graph 8: Graph of C1s signals from FG-CN and FG-NH_2 in high-resolution XPS

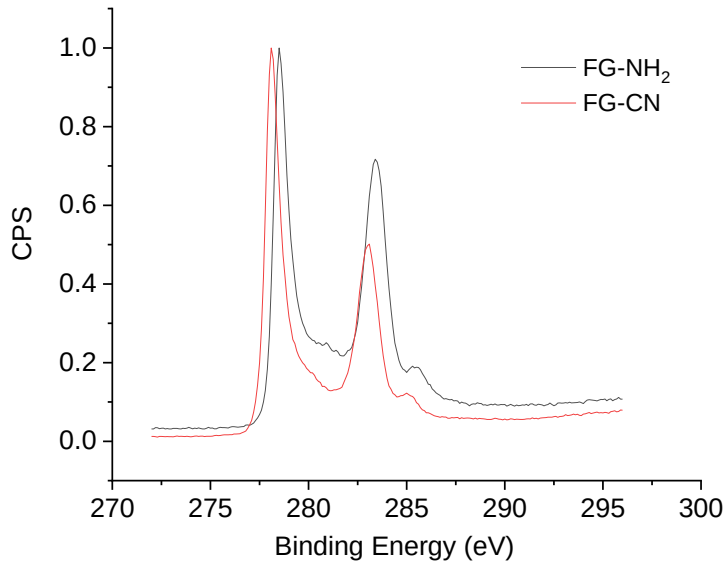

Graph 9: Graph of N1s signals from FG-CN and FG-NH_2 in high-resolution XPS